Sonoma Technology, Inc.

COMPARISONS BETWEEN LIGHT SCATTERING AND FINE-PARTICLE MASS DATA

California Regional $PM_{10}/PM_{2.5}$ Air Quality Study (CRPAQS) Data Analysis Task 1.1a

TECHNICAL MEMORANDUM
STI-902321-2644-TM2

By:
Siana H. Alcorn
L. Willard Richards
Sonoma Technology, Inc.
Petaluma, CA

Prepared for:
California Air Resources Board
Sacramento, CA

July 2005

1360 Redwood Way, Suite C • Petaluma, CA 94954-1169

707/665-9900 • www.sonomatech.com

Sonoma Technology, Inc.

1360 Redwood Way, Suite C
Petaluma, CA 94954-1169
707/665-9900
FAX 707/665-9800
www.sonomatech.com

California Regional PM_{10}/$PM_{2.5}$ Air Quality Study (CRPAQS)
Data Analysis Task 1.1a

COMPARISONS BETWEEN LIGHT SCATTERING AND FINE-PARTICLE MASS DATA

TECHNICAL MEMORANDUM
STI-902321-2644-TM2

By:
Siana H. Alcorn
L. Willard Richards
Sonoma Technology, Inc.
1360 Redwood Way, Suite C
Petaluma, CA 94954-1169

Donald Lehrman
Technical and Business Systems, Inc.
859 Second Street
Santa Rosa, CA 95404

Prepared for:
California Air Resources Board
1001 I Street
Sacramento, CA 95814

July 29, 2005

This page is intentionally blank.

DISCLAIMER

The statements and conclusions in this report are those of the Contractor and not necessarily those of the California Air Resources Board, the San Joaquin Valleywide Air Pollution Study Agency, or its Policy Committee, their employees or their members. The mention of commercial products, their source, or their use in connection with material reported herein is not to be construed as actual or implied endorsement of such products.

This page is intentionally blank.

TABLE OF CONTENTS

Section **Page**

DISCLAIMER iii
LIST OF FIGURES vii
LIST OF TABLES ix

1. INTRODUCTION 1-1

2. SUMMARY OF FINDINGS 2-1

3. METHODS 3-1
   3.1 Data Collection 3-1
   3.2 Data Used 3-2
   3.3 Analysis Methods 3-6

4. RESULTS 4-1
   4.1 Comparison of b_{sp} to $PM_{2.5}$ 4-1
   4.2 Contribution of Coarse Particles to Light Scattering 4-8
   4.3 Dependence on Relative Humidity 4-13

5. RECOMMENDATIONS 5-1

6. REFERENCES 6-1

APPENDIX A: SITE SPECIFIC RELATIONS BETWEEN b_{sp} AND $PM_{2.5}$ A-1

This page is intentionally blank.

LIST OF FIGURES

Figure **Page**

3-1. CRPAQS sites with collocated RR nephelometer and either SFS or MiniVol $PM_{2.5}$ measurements 3-4

4-1. RR nephelometer 24-hour b_{sp} versus SFS $PM_{2.5}$ at the annual and winter intensive Anchor sites 4-1

4-2. RR nephelometer 24-hour b_{sp} versus MiniVol $PM_{2.5}$ at the SJV Satellite sites 4-2

4-3. RR nephelometer 24-hour b_{sp} versus SFS $PM_{2.5}$ at the annual and winter intensive anchor sites stratified by season 4-3

4-4. RR nephelometer 24-hour b_{sp} versus MiniVol $PM_{2.5}$ at the SJV satellite sites 4-3

4-5. RR nephelometer 24-hour b_{sp} versus $PM_{2.5}$ at the desert sites stratified by season 4-7

4-6. November through April hourly light-scattering efficiencies versus RH in the RR nephelometer at Bakersfield 4-13

4-7. December 13, 2000 through February 2, 2001 hourly light-scattering efficiencies versus RH in the RR nephelometer at Angiola 4-14

4-8. Cool season hourly b_{sp} versus BAM $PM_{2.5}$ at Angiola and Bakersfield stratified by RH in the RR nephelometer 4-15

A-1 Scatter plots by site and season of the CRPAQS nephelometer 24-hr average bsp and SFS $PM_{2.5}$ mass concentrations data A-3

A-2 Scatter plots by site and season of the CRPAQS nephelometer 24-hr average b_{sp} and MiniVol $PM_{2.5}$ mass concentrations data A-5

This page is intentionally blank.

LIST OF TABLES

Table		Page
3-1.	CRPAQS sites with collocated RR nephelometer b_{sp} and filter $PM_{2.5}$ measurements	3-5
4-1.	Regression results for the dependence of 24-hour b_{sp} on filter $PM_{2.5}$ for all data and for all data stratified by season	4-4
4-2.	Regression results for the dependence of 24-hour b_{sp} on filter $PM_{2.5}$ when there were more than 10 points included in the regression and the R^2 values were greater than 0.7	4-6
4-3.	Regression results for the dependence of 24-hour b_{sp} on the MiniVol $PM_{2.5}$ in the desert	4-8
4-4.	Regression results for the dependence of 24-hour b_{sp} on $PM_{2.5}$ and PM_c	4-11
4-5.	Regression results for comparison between hourly b_{sp} and BAM $PM_{2.5}$ for cool season data at Angiola and Bakersfield	4-16
4-6.	Regression results for the dependence of hourly b_{sp} on BAM $PM_{2.5}$ and PM_c for the cool season at Angiola and Bakersfield	4-16
A-1.	Regression results for the dependence of 24 hour bsp on filter PM2.5 stratified by site for all data from that site and for data stratified by season	A-1

This page is intentionally blank.

1. INTRODUCTION

California Regional $PM_{10}/PM_{2.5}$ Air Quality Study (CRPAQS) was designed to obtain information needed to develop equitable and effective control measures for particulate matter (PM) in the atmosphere of the San Joaquin Valley (SJV) (Watson et al., 1998). The field program plan included the measurement of light scattering by particles (b_{sp}) at nearly all monitoring sites because the measurement is cost-effective, can be made with high time resolution, and previous studies have shown that b_{sp} can be highly correlated with the mass concentration of particles in the atmosphere with a diameter smaller than 2.5 μm ($PM_{2.5}$) (Richards et al., 1999 present data for the SJV). However, it is known that the correlation between b_{sp} and $PM_{2.5}$ depends on the PM composition and size distribution, which can vary with time and location (Lowenthal et al., 1995). Therefore, collocated filter measurements of $PM_{2.5}$ were used to develop correlations appropriate for each site and meteorological regime that will allow estimation of $PM_{2.5}$ from the b_{sp} measurements. The dense spatial coverage and high time resolution of these data should enable them to play a key role in the analysis of the CRPAQS data.

The CRPAQS data include b_{sp} measurements by 56 Radiance Research Model 903 Integrating Nephelometers (RR nephelometers) with 5-minute time resolution at a total of 77 sites. Measurements at some of these sites were made only during special or intensive studies. Continuous measurements were made for a year or more at 15 of these sites (Technical and Business Systems and Parsons Engineering Science, 2002; Wittig et al., 2003). An extended abstract by Richards et al. (2001) describes the RR nephelometer and the Standard Operating Procedure for CRPAQS describes its operation (Richards, 2002b). The RR nephelometers were operated without a size selective inlet and with a "smart heater" that heated only as needed to keep the relative humidity (RH) in the nephelometer scattering chamber below about 72%. Technical and Business Systems, Inc. (T&B Systems) reported data recovery rates greater than 90% for most satellite sites, and above 97% for many sites during the winter intensive near the end of the field study (Technical and Business Systems and Parsons Engineering Science, 2002).

This report presents the results from the comparison of b_{sp} measured at 48 sites with collocated filter measurements of $PM_{2.5}$. These results make it possible to estimate $PM_{2.5}$ from the b_{sp} data. The estimates are much more reliable in the cool season (November through April), when most of the PM is $PM_{2.5}$. The estimates are a qualitative indicator of PM during the warm season (May through October), when dust is a major component of the PM and a significant contributor to the measured b_{sp}. Site-specific correlations between b_{sp} and $PM_{2.5}$ have been developed for each site with adequate data for use in computer model evaluation and validation or other detailed analyses. Study average correlations have been calculated for the cool season, for use in more general analyses.

This page is intentionally blank.

2. SUMMARY OF FINDINGS

The following list enumerates the key findings from this and prior investigations of the performance of the RR nephelometers and the relation between RR nephelometer b_{sp} readings and PM concentrations during CRPAQS.

1. The b_{sp} data were found to be complete and of high quality. A review of the field calibration data for b_{sp} at the satellite sites indicated that there would be little benefit from applying calibrations. The database contains the b_{sp} values recorded by the RR nephelometers at the satellite sites, and these were used in these analyses without modification. Calibration data were applied to the anchor site b_{sp} data before submission to the database, and these values were also used in these analyses without modification.
2. Both collocated measurements during special studies and field data from nearby sites indicate the b_{sp} readings are precise and repeatable.
    2.1. The analysis of data from the intercomparison of four RR nephelometers collocated at the Angiola site after the end of the field study provides quantitative data on the repeatability of the b_{sp} measurements (Richards, 2002a). Intercomparison data are also reported by Technical and Business Systems, Inc. and Parsons Engineering Science, Inc. (2002).
    2.2. Comparisons of the b_{sp} data from the FREM (Fresno Motor Vehicle) and FRES (Fresno Residential) sites not reported here show that b_{sp} data from at least some field sites have a repeatability comparable to that observed during the Angiola intercomparison. These sites are separated by 1.4 km, and when differences between the two measurements occur, they can be attributed to local effects.
3. Field audit and calibration data indicate that the b_{sp} readings are an accurate measure of the b_{sp} of the particles in the nephelometer scattering chamber. When 24 outliers were removed, the remaining 367 calibrations and audits of 52 nephelometers at 71 Satellite sites gave an average zero of 0.4 ± 1.4 Mm^{-1} and an average span slope of 0.99 ± 0.05 (Richards et al., 2001).
4. Several factors affected the relation between the b_{sp} in the RR nephelometer scattering chamber and the ambient b_{sp}.
    4.1. The sample air flow passed through a "smart heater" on the nephelometer inlet, which heated the sample air only when the RH in the scattering chamber exceeded 65% and prevented the RH in the scattering chamber from exceeding about 72%.
        4.1.1. The smart heater successfully protected the nephelometer from accumulating liquid water on the internal optics during dense fog events.
        4.1.2. A small fraction of the b_{sp} data recorded when the RH in the nephelometer was near 70% have a significantly higher value than expected from the $PM_{2.5}$. During times when collocated ambient liquid water content data were available, most, but not all, of these anomalously high b_{sp} values were recorded when fog was present.

4.2. The RR nephelometers did not have size-selective inlets. It is believed that $PM_{2.5}$ was sampled with high efficiency. It is expected that the sampling efficiency for coarse particles was smaller and decreased with increasing particle size, but the sampling efficiency has not been characterized. Light scattering by both coarse and fine particles is included in all CRPAQS RR nephelometer b_{sp} data.

5. Linear regression analyses were used to relate b_{sp} and $PM_{2.5}$. The regression slope is an estimate of the light-scattering efficiency of $PM_{2.5}$.

   5.1. During the cool season (November through April), when the contribution of dust to the PM concentrations is small, the recommended light-scattering efficiency for estimating $PM_{2.5}$ from b_{sp} varies linearly from approximately 4.0 m^2/g when the RH in the nephelometer is 20% to about 5.7 m^2/g at 70% RH. For individual readings, the standard error in the light-scattering efficiency is roughly 1 m^2/g.

   5.2. During the warm season (May through October), dust is a major and variable component of PM in the SJV. The light-scattering efficiency of the $PM_{2.5}$ tail of the dust particle size distribution is much smaller than for accumulation mode particles, so the b_{sp} data provide only a semi quantitative indicator of PM during the warm season.

   5.3. $PM_{2.5}$ greater than about 50 $\mu g/m^3$ were seldom observed during the warm season, while 24-hour $PM_{2.5}$ up to 179 $\mu g/m^3$ were observed during the cool season. Thus, the estimates of the $PM_{2.5}$ from b_{sp} readings are most reliable during the season when high $PM_{2.5}$ readings occur.

   5.4. During dust events in the desert, the light-scattering efficiency calculated for $PM_{2.5}$ was sometimes less than 1 m^2/g. Since some of the b_{sp} is caused by light scattering by coarse particles, the actual light-scattering efficiency of the $PM_{2.5}$, which was mostly the fine particle tail of the dust particle size distribution, was appreciably less than 1 m^2/g.

6. Regression analyses were performed separately for all sites with sufficient data to support this analysis, and the results for each site are reported separately. This permits using site-specific regression results to estimate $PM_{2.5}$ from b_{sp} for such tasks as computer model evaluation and validation

7. The above findings indicate that the RR nephelometer b_{sp} measurements met the objectives set for them in the program plan (Watson et al., 1998). These findings provide good estimates of $PM_{2.5}$ with 5-minute time resolution at dozens of sites in and near the SJV during the season in which elevated $PM_{2.5}$ readings occur.

8. The following uses of the b_{sp} data are recommended:

   8.1. It is recommended that the b_{sp} data measured during the cool season (November through April) in the SJV be used to estimate $PM_{2.5}$. For general analyses, regression equations derived from all data can be used. The site-specific relations can be used for more demanding analyses.

   8.2. In careful work, it should be recognized that there is a greater uncertainty in the relation between b_{sp} and $PM_{2.5}$ when the RH measured in the nephelometer is above 65% than when the RH is lower.

8.3. During the warm (dry) season, the b_{sp} data provide a semi-quantitative indication of PM concentrations.

8.4. The usefulness of warm (dry) season b_{sp} data for model evaluation and validation would be increased if the model simulates the accumulation mode and dust concentrations, assigns different light-scattering efficiencies to these two particle fractions, then compares the reconstructed b_{sp} with the observations.

This page is intentionally blank.

3. METHODS

3.1 DATA COLLECTION

Radiance Research Model 903 Integrating Nephelometers (RR nephelometers) were used to collect the CRPAQS b_{sp} data. These nephelometers were operated without size selective inlets and with smart heaters to control the RH in the sampled air. The sample air was heated only when the RH exceeded 65%, and the heater controller did not allow the RH measured in the nephelometer to exceed 72%.

A description of the RR nephelometer has been prepared by Richards et al. (2001). Copies of this extended abstract are available on request, preferably as an e-mail attachment. The RR nephelometer and its operation are also described in the CRPAQS Standard Operating Procedure (Richards, 2002b) and in the report on the satellite site field operations (Technical and Business Systems and Parsons Engineering Science, 2002)

The nephelometers were operated at the satellite sites by T&B Systems (Technical and Business Systems and Parsons Engineering Science, 2002) and at most anchor sites by Sonoma Technology, Inc. (STI) (Wittig et al., 2003; Hafner et al., 2003; Hyslop et al., 2003). The overall field program plan is reported by Watson et al. (1998). The nephelometers were calibrated approximately every two weeks and performance audits were also conducted. The calibration and performance audit data are in the above reports of the field operations.

All b_{sp} data were reviewed before submission to the CRPAQS database to remove or flag data recorded during calibrations, instrument malfunctions, etc. STI applied calibration factors to all anchor site data as appropriate, and reported calibrated data to the CRPAQS database. T&B Systems did not apply calibration factors to the b_{sp} data from the satellite sites, but did report the data from the calibrations and audits. The satellite site calibration data were reviewed as part of the work reported here and it was determined that the calibration corrections were small enough that there would be little benefit from applying them. The work reported here did not discover any b_{sp} data that needed to be corrected, so no corrections were submitted to the database. Corrections to filter PM data were submitted.

The sample air flow configuration of the nephelometers was changed in December 2000. Initially, the nephelometer was operated as it was designed with the RH sensor for the smart heater on the sample air inlet. Unfortunately, this allowed the possibility at low ambient temperatures that heat loss from the body of the nephelometer could cool the air in the scattering chamber, with the result that the RH there would be higher than at the RH sensor. It was feared that this inadvertent sample air cooling was contributing to some cases where the light-scattering efficiency of the $PM_{2.5}$ was higher than expected. Therefore, the sample air flow through the nephelometer was reversed, so it entered the nephelometer through the port that was normally the outlet and flowed past the RH sensor after leaving the scattering chamber. Also, the body of the nephelometer was enclosed in a sheet of foam thermal insulation. The date of this change is documented in the reports of the field operations.

An intercomparison was conducted after the end of the field study to determine the effect on the measured b_{sp} of this change in the sample air flow and thermal insulation. An analysis of

the results of this intercomparison has been reported by Richards (2002a). These data provide further confirmation that the b_{sp} data can be highly repeatable, and showed that the change in nephelometer configuration had a small, but repeatable effect on the data. A dense fog event did not occur during this intercomparison, so the effect of the configuration change on the b_{sp} data during dense fogs was not determined.

3.2 DATA USED

The b_{sp} and filter $PM_{2.5}$ data can be compared only at sites where nephelometers were collocated with filter samplers. **Figure 3-1** shows the sites where these comparisons are possible. The sites are classified as being within or outside of the SJV. The sites outside the SJV are Olancha, China Lake, Edwards, Tehachapi Pass, Bodega Bay, San Francisco, and Sierra Nevada Foothills. Sites as far north as Pleasant Grove are included in the SJV classification. **Table 3-1** lists the sites in Figure 3-1 and the time periods for which collocated data are available. The Carrizo Plain site should have been classified as outside the SJV, but it is believed that including it in the SJV sites had little effect on the results.

The annual and winter intensive anchor sites, Angiola, Bakersfield California Ave., Fresno First Street, Sierra Nevada Foothills, and Bethel Island had RR nephelometer measurements collocated with Desert Research Institute (DRI) $PM_{2.5}$ sequential filter samplers (SFS). Thirty-three satellite sites had RR nephelometers collocated with $PM_{2.5}$ MiniVols. On some days, these samplers measured $PM_{2.5}$ and on other days they measured the mass concentration of particles in the atmosphere smaller than 10-μm diameter (PM_{10}). Only 13 site-days had simultaneous MiniVol PM_{10} and $PM_{2.5}$ filter measurements during the CRPAQS. These were at Corcoran (9 days), Modesto (2 days), and Visalia (2 days). Therefore, there was not sufficient filter data to determine the simultaneous concentrations of fine and coarse particles for use in regression analyses.

Angiola, Bakersfield, Fresno, Corcoran, and Edwards Air Force Base had $PM_{2.5}$ and PM_{10} Beta Attenuation Monitors (BAMs) collocated with the CRPAQS $PM_{2.5}$ filter samplers and RR nephelometers. The difference between PM_{10} and $PM_{2.5}$ provided estimates of the mass concentrations of particles in the atmosphere between 2.5- and 10-μm diameter (PM_c). The BAM data were reported with hourly time resolution, and therefore had adequate time resolution to evaluate the effect of RH on the relation between b_{sp} and the PM data.

Dichotomous samplers (Dichots) and Federal Reference Method (FRM) PM_{10} and $PM_{2.5}$ samplers were collocated with the $PM_{2.5}$ SFS and RR nephelometers at the Bakersfield and Fresno anchor sites. FRM PM_{10} and $PM_{2.5}$ samplers were collocated with the $PM_{2.5}$ MiniVols and RR nephelometers at Clovis, Corcoran, Modesto, Oildale, Stockton, and Visalia. At Modesto and Stockton, Dichots were also collocated with the $PM_{2.5}$ MiniVols and RR nephelometers. Only sites where RR nephelometers were collocated with the SFS or MiniVol filter $PM_{2.5}$ samplers are discussed in this report. This criterion excluded data from the Sacramento Del Paso site because no SFS or MiniVol $PM_{2.5}$ mass measurements were made at the site.

The work described in this report was started in February 2003, early in the CRPAQS data analysis effort. Therefore, most of the data were acquired from data sets submitted to the California Air Resources Board (ARB) for inclusion in the Central California Air Quality Studies (CCAQS) database but not yet readily available there. Most of the RR nephelometer data were acquired from STI's and T&B System's internal databases on a 5-minute time base. The Fresno First Street and portions of the Corcoran nephelometer data were acquired via ARB staff. The CRPAQS filter data analyzed by DRI were acquired through Liz Niccum in the format received for submittal into the CCAQS database. The BAM, FRM, and Dichot data were acquired through the CCAQS database and ARB staff. It is our understanding that in all cases where data used for this analysis were acquired through means other than directly from the CCAQS database, the data differ from the CCAQS database in format alone.

The 5-minute b_{sp} data were averaged into hourly averages for comparison with the BAM data. The hourly averages were averaged into 24-hr values for comparisons with the filter data. A 75% data completeness criterion was imposed at each time averaging step. If this criterion was not met, the average was listed as missing.

Most filter data were reported as 24-hr averages. During some intensive operation periods when shorter filter sampling times were used, the filter data were averaged to obtain 24-hr values. Due to an oversight, no data completeness criterion was applied when averaging the filter data into 24-hr values. A 75% data completeness criterion would have eliminated one day of data, December 15, 2000, at Bethel Island and would not have significantly changed any analysis results.

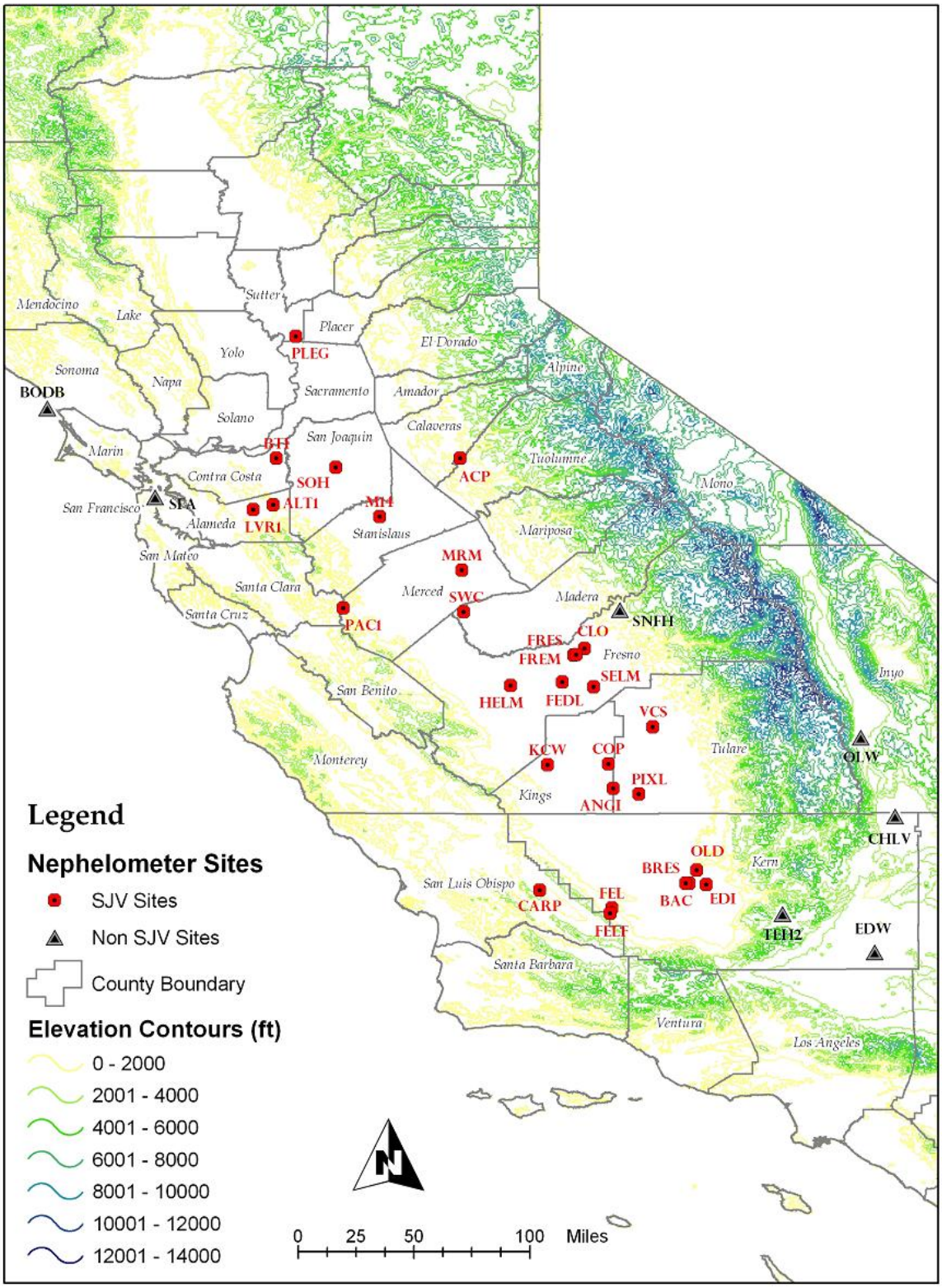

Figure 3-1. CRPAQS sites with collocated RR nephelometer and either SFS or MiniVol $PM_{2.5}$ measurements.

Table 3-1. CRPAQS sites with collocated RR nephelometer b_{sp} and filter $PM_{2.5}$ measurements. The time period of available collocated data is also listed.

Site	Site Code	$PM_{2.5}$ Filter Sampler	Period with Collocated b_{sp} and Filter $PM_{2.5}$	
Angiola	ANGI	SFS	2/1/00	2/3/01
Bakersfield California Ave.	BAC	SFS	1/6/00	2/4/01
Fresno First St.	FSF	SFS	1/21/00	2/3/01
Bethel Island	BTI	SFS	12/1/00	2/3/01
Sierra Foothills	SNFH	SFS	12/1/00	2/3/01
Altamont Pass	ALT	MiniVol	1/31/00	2/1/01
Angels Camp	ACP	MiniVol	12/8/00	2/3/01
Bakersfield Residential	BRES	MiniVol	12/2/00	2/3/01
Bethel Island	BTI	MiniVol	3/19/00	1/31/01
Bodega Bay	BODG	MiniVol	12/26/99	2/3/01
China Lake	CHLV	MiniVol	3/7/00	1/31/01
Clovis	CLO	MiniVol	12/14/00	2/3/01
Corcoran	COP	MiniVol	10/9/00	2/3/01
Carrizo Plain	CARP	MiniVol	7/5/00	1/31/01
Dairy Feedlot	FEDL	MiniVol	7/11/00	2/3/01
Edison	EDI	MiniVol	12/8/00	2/3/01
Edwards	EDW	MiniVol	2/12/00	1/31/01
Fellows	FEL	MiniVol	1/31/00	2/3/01
Fellows Foothills	FELF	MiniVol	3/19/00	2/3/01
Fresno Motor Vehicle	FREM	MiniVol	1/25/00	2/3/01
Fresno Residential	FRES	MiniVol	1/31/00	2/3/01
Helm	HELM	MiniVol	12/2/00	2/3/01
Kettleman City	KCW	MiniVol	12/2/00	2/3/01
Livermore	LVR	MiniVol	11/20/00	2/3/01
Merced	MRM	MiniVol	12/2/00	2/3/01
Modesto	M14	MiniVol	11/14/00	2/3/01
Oildale	OLD	MiniVol	12/2/00	1/31/01
Olancha	OLW	MiniVol	3/7/00	2/3/01
Pacheco	PAC1	MiniVol	2/6/00	1/31/01
Pixley Wildlife	PIXL	MiniVol	1/31/00	2/3/01
Pleasant Grove	PLEG	MiniVol	12/2/00	1/31/01
San Francisco	SFA	MiniVol	11/20/00	1/31/01
Sierra Nevada Foothills	SNFH	MiniVol	3/19/00	2/3/01
Selma Airport	SELM	MiniVol	1/31/00	1/31/01
Stockton	SOH	MiniVol	12/2/00	2/3/01
Southwest Chowchilla	SWC	MiniVol	12/2/00	2/3/01
Tehachapi Pass	TEH2	MiniVol	3/25/00	2/3/01
Visalia	VCS	MiniVol	12/2/00	2/3/01

3.3 ANALYSIS METHODS

Linear regression analyses were used to relate 24-hr average RR nephelometer b_{sp} data to collocated filter SFS and MiniVol $PM_{2.5}$. The data were stratified by both site and season. Two seasons were used for this stratification: the cool season, November through April, and the warm season, May through October.

As mentioned above, there were only 13 days when it was possible to determine PM_c from the SFS and MiniVol data. Therefore, the FRM, Dichot, as well as 24-hr average BAM PM_{10} and $PM_{2.5}$ data were used to quantify PM_c. These PM_c data were combined with the SFS or MiniVol $PM_{2.5}$ and b_{sp} data for regression analyses with b_{sp} as the dependent variable and both $PM_{2.5}$ and PM_c as the independent variables.

Sites that had RR nephelometer b_{sp} data collocated with BAM PM_{10} and BAM $PM_{2.5}$ were analyzed separately on an hourly basis. Hourly comparisons between b_{sp}, $PM_{2.5}$ and PM_c were made at Angiola, Bakersfield, Fresno, Corcoran, and Edwards. The effect of RH measured in the nephelometer on the relation between b_{sp} and $PM_{2.5}$ was evaluated using hourly BAM data from Bakersfield and Angiola. It was not possible to use filter data to explore RH effects because of the wide variations in RH during the filter sampling periods.

4. RESULTS

4.1 COMPARISON OF b_{sp} TO $PM_{2.5}$

The relationships between the RR nephelometer b_{sp} data and PM concentrations in the CRPAQS data are evaluated in this section. These relationships have been explored in a very large number of previous studies (Watson, 2002), and it is typically found that b_{sp} is well correlated with $PM_{2.5}$ and less well correlated with PM_{10} (see, for example, Lowenthal et al., 1995). The relationship depends on the PM size distribution, so has been found to vary among measurement sites and seasons. The work in this report adds to previous work by developing these relationships for the PM concentrations, compositions, and size distributions that occurred in and near the SJV during the CRPAQS field study. A key purpose of this work is to develop "customized" relationships that can be used for the interpretation of the CRPAQS data as well as for the evaluation and validation computer models that simulate PM concentrations in the SJV.

The scatter diagrams in **Figures 4-1 and 4-2** provide an overview of the relation between the 24-hour b_{sp} and $PM_{2.5}$ values. Data from all sites for both seasons are combined for each of the two PM measurement methods. Figure 4-1 shows all data from the annual and winter anchor sites using $PM_{2.5}$ data from the SFS. All data from the SJV satellite sites, where $PM_{2.5}$ was measured by the MiniVol, are shown in Figure 4-2. Factors that contribute to the difference between these two results are differences in the PM composition and size distribution at the anchor and satellite sites and differences between the PM sampling methods.

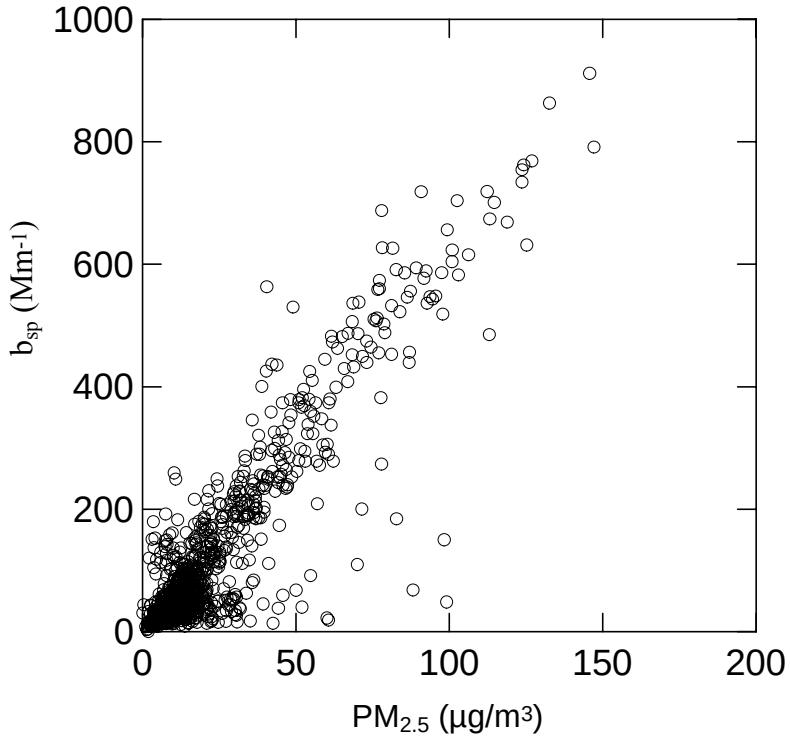

Figure 4-1. RR nephelometer 24-hour b_{sp} versus SFS $PM_{2.5}$ at the annual and winter intensive Anchor sites.

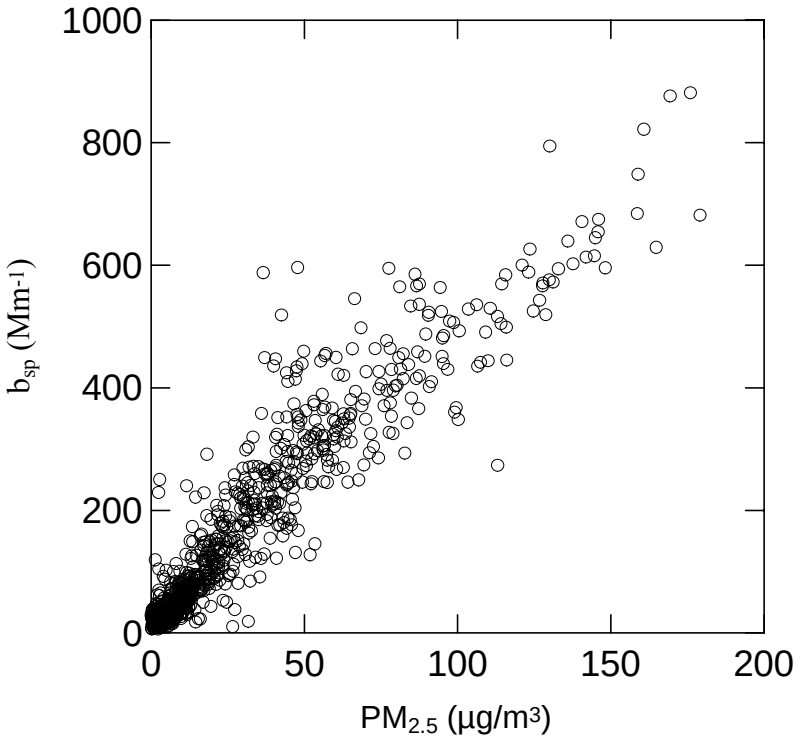

Figure 4-2. RR nephelometer 24-hour b_{sp} versus MiniVol $PM_{2.5}$ at the SJV Satellite sites.

It is well established that the PM composition and size distribution in the SJV depend strongly on the season. During the summer, dust is the major component of PM_{10}. During the winter, the rains suppress the dust and the stagnant conditions favor the accumulation of high concentrations of $PM_{2.5}$. **Figures 4-3 and 4-4** show the data in Figures 4-1 and 4-2 stratified into data for the warm season, May through October, and a cool season, November through April. Using a regression model that assumes that b_{sp} is a linear function of $PM_{2.5}$ gives the results in **Table 4-1**. The equation for this model is

$$b_{sp} = A + E_{2.5}\, PM_{2.5} \qquad \textbf{(4-1)}$$

where A is the intercept and the slope $E_{2.5}$ is assumed to be a constant and is an estimate of the light-scattering efficiency of the $PM_{2.5}$. Table 4-1 also contains regression results in which the intercept is forced to be zero.

The estimate of the light-scattering efficiency based on Equation 4-1 is biased by the fact that the b_{sp} measured by the RR nephelometer responds to light scattering by both the fine and coarse particles that enter the scattering chamber, while $PM_{2.5}$ is a measure of only the fine particles. Additional information on the effect of coarse particles on b_{sp} is presented in Section 4.2.

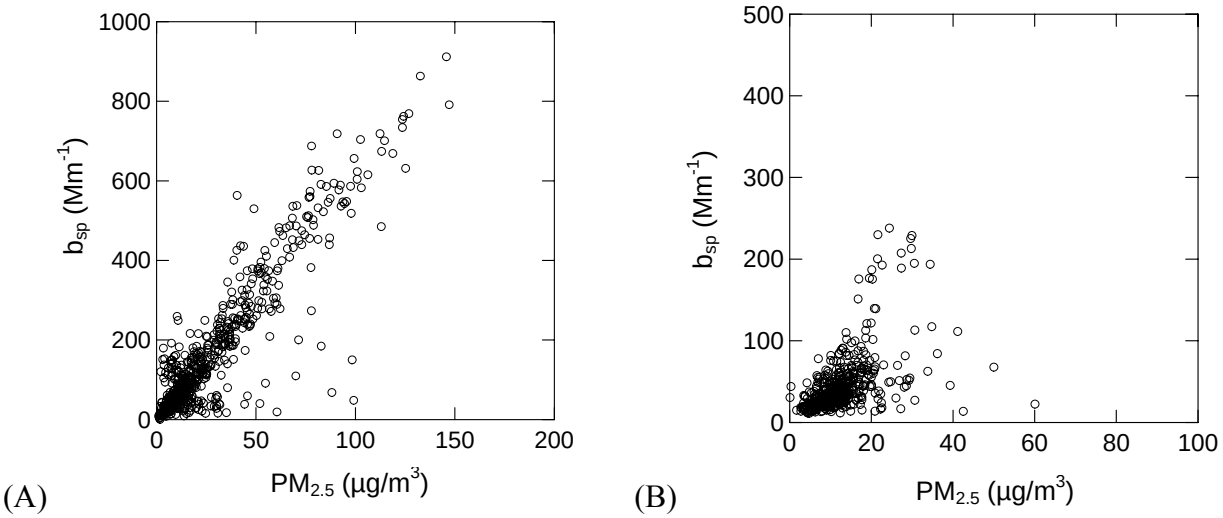

Figure 4-3. RR nephelometer 24-hour b_{sp} versus SFS $PM_{2.5}$ at the annual and winter intensive anchor sites stratified by season. Cool season, November – April, data are in Figure A and warm season, May – October, data in Figure B.

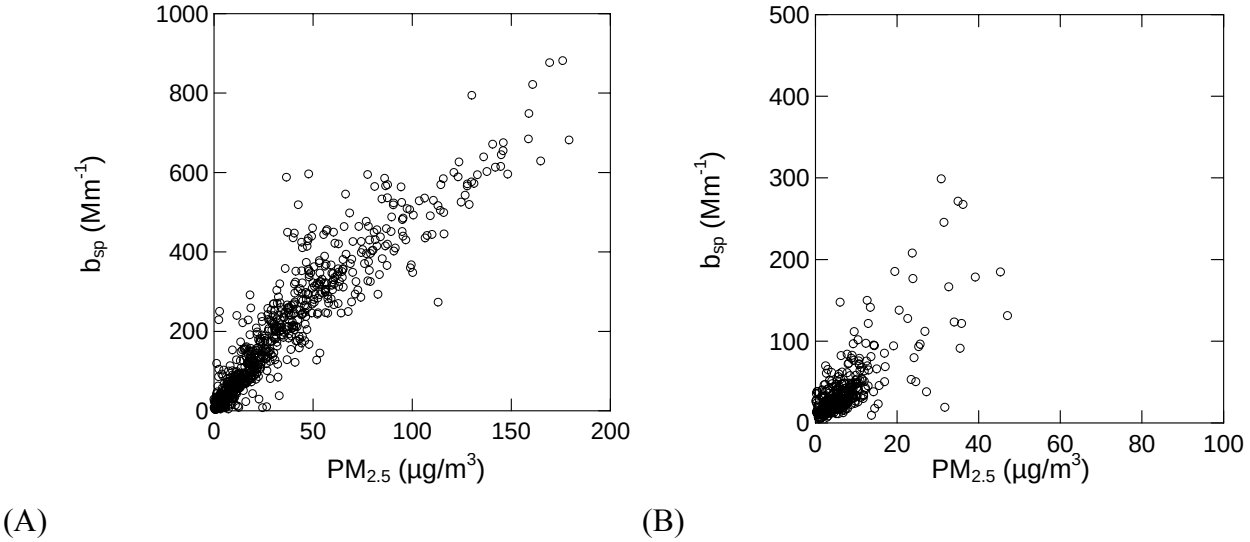

Figure 4-4. RR nephelometer 24-hour b_{sp} versus MiniVol $PM_{2.5}$ at the SJV satellite sites. Cool season, November – April, data are in Figure A and warm season, May – October, data in Figure B.

The warm season data in Figures 4-3 and 4-4 show that the 24-hour $PM_{2.5}$ rarely exceeded 40 µg/m^3 during this time of year. Also, the correlation between b_{sp} and $PM_{2.5}$ is weaker than during the cool season. Much of the deviation of the warm season data from the regression line for all data is caused by points with a low light-scattering efficiency, i.e., a b_{sp} that is smaller than expected from the observed $PM_{2.5}$. This deviation is attributed to dust. The

tail of the dust particle size distribution that extends into the $PM_{2.5}$ size range is mostly composed of particles with a diameter larger than 1 μm, which have smaller light-scattering efficiencies than the accumulation mode particles. The RR nephelometer b_{sp} is a relatively poor predictor of $PM_{2.5}$ during the warm season because: (1) much of the PM_{10} is dust; (2) the relative amounts of dust and accumulation mode aerosol are quite variable, and (3) the light-scattering efficiency of the $PM_{2.5}$ tail of the dust particle size distribution is much less than the light-scattering efficiency of the accumulation mode aerosol. During the warm season, b_{sp} provides a qualitative indicator of PM concentrations.

Table 4-1. Regression results for the dependence of 24-hour b_{sp} on filter $PM_{2.5}$ for all data and for all data stratified by season.

Category	Sites ($PM_{2.5}$ Measurement Method)	Intercept Mm^{-1}	Standard Error Mm^{-1}	Slope m^2/g	Standard Error m^2/g	Number of Data Points	R^2
All Data	All Annual and Winter Anchor (SFS)	-11.0	2.7	5.89	0.08	1067	0.82
All Data		0.0	Forced	5.65	0.06	1067	0.82
Cool		5.7	4.2	5.77	0.11	623	0.83
Cool		0.0	Forced	5.87	0.07	623	0.83
Warm		12.3	3.1	2.65	0.21	444	0.26
Warm		0.0	Forced	3.38	0.10	444	0.23
All Data	All SJV Satellite[a] (MiniVol)	19.2	2.0	4.85	0.05	1174	0.89
All Data		0.0	Forced	5.16	0.04	1174	0.88
Cool		31.2	3.0	4.71	0.06	792	0.88
Cool		0.0	Forced	5.16	0.04	792	0.86
Warm		8.4	1.9	4.25	0.18	382	0.58
Warm		0.0	Forced	4.85	0.13	382	0.56

[a] All satellite sites except Edwards, Olancha, Tehachapi Pass, Bodega Bay, San Francisco, China Lake, and Sierra Nevada Foothills.

$PM_{2.5}$ in the 50 to 175 $\mu g/m^3$ range occurs almost exclusively during the cool season, when the PM_{10} is mostly $PM_{2.5}$. The data with these high values of b_{sp} and $PM_{2.5}$ dominate the regression results for the data for all seasons. Therefore, the regression results for all data are similar to those for the cool season. The b_{sp} to SFS $PM_{2.5}$ comparison from the anchor sites yields a light-scattering efficiency of 5.9 ± 0.1 m^2/g using all data, and 5.8 ± 0.1 m^2/g using only the cool season data. In both cases, about 82% of the variation in the b_{sp} data can be explained by the variation in the $PM_{2.5}$ data. The b_{sp} to MiniVol $PM_{2.5}$ comparison yields somewhat smaller scattering efficiencies of 4.8 ± 0.1 m^2/g using all data and 4.6 ± 0.1 m^2/g using only cool season data. In both cases, about 87% of the variation in b_{sp} is explained by the regression.

Site-specific regressions were created to assess the spatial variability of the relationship between b_{sp} to $PM_{2.5}$. The scatter plots for all sites using all data and by season are shown in the Appendix. The light-scattering efficiencies as calculated from b_{sp} and MiniVol $PM_{2.5}$ at the

satellite SJV sites range from 3.0 to 6.3 m^2/g during the cool season and from -0.4 to 7.2 m^2/g during the warm season. Scattering efficiencies calculated from the anchor sites with the SFS $PM_{2.5}$ data; Angiola, Bakersfield, Fresno, Bethel Island, and Sierra Nevada Foothills, range from 5.4 to 6.1 m^2/g in the cool season. Data from the three annual anchor sites are available in the warm season and the scattering efficiencies range from around 2 m^2/g at Angiola and Bakersfield to 5.7 m^2/g at Fresno. The variability of regression slopes during the warm season indicates that it is not possible to reliably estimate $PM_{2.5}$ from b_{sp} during this season.

The correlation between b_{sp} and $PM_{2.5}$ also varies significantly between sites. The regression results by season for all sites are summarized in the Appendix. **Table 4-2** summarizes the regression results of the site specific comparisons between b_{sp} and filter $PM_{2.5}$ for sites where the more than 70% of variance in the b_{sp} data is explained by the regression. In all cases except Selma Airport, a rural agricultural site, and Olancha, a desert site, the cool season data provides stronger correlation than the warm season.

The seasonal dependence of b_{sp} on $PM_{2.5}$ at the desert sites, Olancha, China Lake, and Edwards Air Force Base, is different from seasonal dependence in the SJV. These sites are shown by triangles at the right side of Figure 3-1. **Figure 4-5** shows scatter plots of the b_{sp} against $PM_{2.5}$ by season and **Table 4-3** summarizes the regression results. The warm season data are more highly correlated than the cool season data at all three desert sites and are more like the cool season data in the SJV.

Table 4-2. Regression results for the dependence of 24-hour b_{sp} on filter $PM_{2.5}$ when there were more than 10 points included in the regression and the R^2 values were greater than 0.7.

Category	Site	Intercept Mm^{-1}	Standard Error Mm^{-1}	Slope m^2/g	Standard Error m^2/g	Number of Data Points	R^2	$PM_{2.5}$ Measurement
Cool	Angiola	12.9	11.0	5.39	0.29	139	0.72	SFS
Cool	Bakersfield	-19.7	9.0	6.10	0.19	192	0.84	SFS
Cool	Fresno	30.1	6.3	5.65	0.15	169	0.89	SFS
Cool	Bethel Island	-1.1	6.4	6.13	0.24	59	0.92	SFS
Cool	Sierra Foothills	-6.1	4.5	5.86	0.20	64	0.94	SFS
Cool	Altamont Pass	13.5	4.4	4.69	0.23	38	0.92	MiniVol
Cool	Bakersfield Residential	50.5	17.7	4.16	0.21	23	0.95	MiniVol
Cool	Bethel Island	3.1	8.4	6.27	0.32	17	0.96	MiniVol
Cool	Clovis	93.1	39.3	4.49	0.58	19	0.78	MiniVol
Cool	Corcoran	96.3	19.8	4.11	0.32	26	0.87	MiniVol
Cool	Edison	101.7	27.8	3.82	0.35	22	0.86	MiniVol
Cool	Fellows	24.6	9.3	3.00	0.24	32	0.84	MiniVol
Warm		9.2	2.5	1.88	0.31	16	0.73	MiniVol
Cool	Fellows Foothills	20.2	12.9	4.06	0.36	27	0.83	MiniVol
Cool	Fresno Motor Vehicle	27.9	12.2	4.49	0.18	42	0.94	MiniVol
Warm		-14.7	7.0	6.21	0.70	30	0.74	MiniVol
Cool	Fresno Residential	30.7	13.6	4.78	0.20	36	0.94	MiniVol
Cool	Helm	54.7	21.7	4.66	0.53	24	0.78	MiniVol
Cool	Kettleman City	35.7	11.1	4.60	0.26	23	0.94	MiniVol
Cool	Livermore	17.7	10.7	4.48	0.31	26	0.90	MiniVol
Cool	Merced	78.5	30.6	5.39	0.63	24	0.77	MiniVol
Cool	Modesto	13.6	8.3	4.95	0.15	22	0.98	MiniVol
Cool	Oildale	18.1	40.5	4.49	0.58	11	0.87	MiniVol
Warm	Olancha	0.9	1.4	4.47	0.16	23	0.97	MiniVol
Cool	Pacheco Pass	18.6	7.2	5.26	0.45	27	0.85	MiniVol
Cool	Pixley Wildlife	66.2	15.6	4.02	0.27	39	0.85	MiniVol
Cool	Pleasant	17.3	21.3	6.31	0.93	11	0.84	MiniVol
Cool	Sierra Nevada Foothills	1.1	9.3	6.73	0.62	28	0.82	MiniVol
Cool	Selma Airport	51.2	17.9	5.01	0.37	36	0.84	MiniVol
Warm	Selma Airport	-16.5	6.3	7.20	0.58	28	0.86	MiniVol
Cool	Stockton	19.2	21.4	4.70	0.49	24	0.81	MiniVol
Cool	SW Chowchilla	39.8	11.5	5.16	0.29	23	0.94	MiniVol
Cool	Visalia	81.7	31.0	4.16	0.44	24	0.80	MiniVol

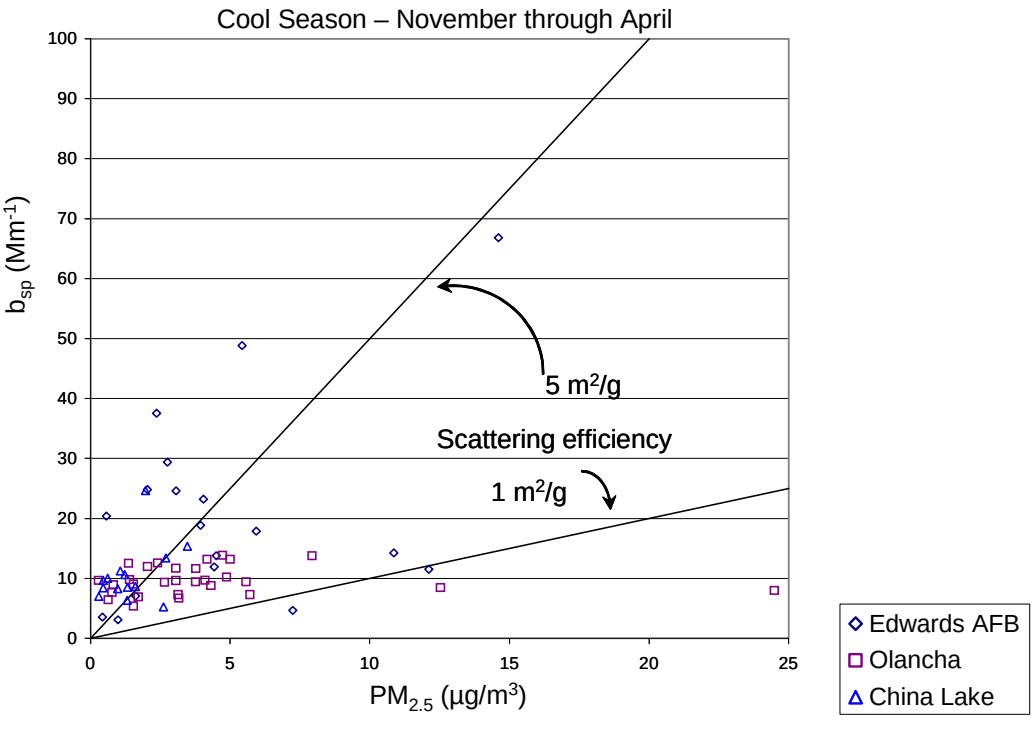

(A)

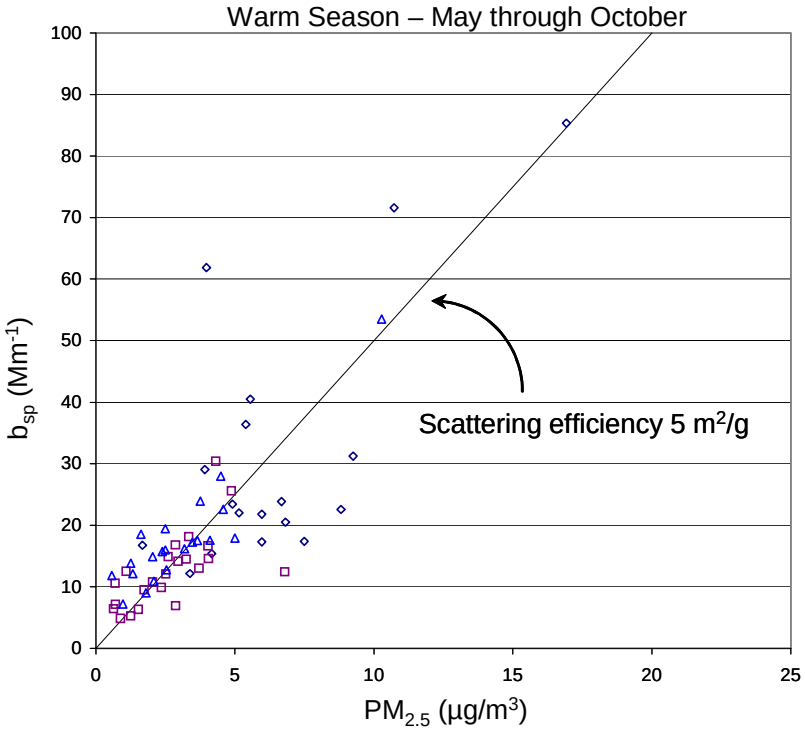

(B)

Figure 4-5. RR nephelometer 24-hour b_{sp} versus $PM_{2.5}$ at the desert sites stratified by season.

Table 4-3. Regression results for the dependence of 24-hour b_{sp} on the MiniVol $PM_{2.5}$ in the desert.

Category	Site	Intercept Mm^{-1}	Standard Error Mm^{-1}	Slope m^2/g	Standard Error m^2/g	Number of Data Points	R^2
All Data	China Lake	5.22	1.20	4.05	0.39	35	0.76
Cool		7.66	2.32	1.99	1.36	14	0.15
Warm		5.11	1.55	4.20	0.42	21	0.84
All Data	Edwards	10.58	4.91	2.80	0.72	36	0.31
Cool		13.65	5.85	1.57	0.94	18	0.15
Warm		5.10	8.15	4.09	1.12	18	0.46
All Data	Olancha	1.37	2.44	3.08	0.33	52	0.64
Cool		9.75	0.60	0.00	0.10	29	0.00
Warm		0.90	1.38	4.47	0.16	23	0.97

Other studies have shown that transport of smog from the Los Angeles Basin and the SJV to the desert is much more common during the warm season, when transport mechanisms are more developed, than during the cool season. This provides a reasonable explanation for the observation of scattering efficiencies during the warm season at the desert sites that are similar to those observed in the cool season in the SJV. It is believed that cool season data near the 1 m^2/g light-scattering efficiency line in Figure 4-5 are caused by dust events, but this has not been confirmed. One data point indicates that the light-scattering efficiency can be less than 0.5 m^2/g. Because b_{sp} includes the light scattered by both coarse and fine particles, this point, if it is correct, indicates that the light-scattering efficiency of the $PM_{2.5}$ fraction of dust can be less than 0.5 m^2/g.

4.2 CONTRIBUTION OF COARSE PARTICLES TO LIGHT SCATTERING

Table 4-4 shows that several types of measurements were used to quantify 24-hour PM_c for use in estimating the contribution of PM_c to b_{sp}. With one exception, the use of FRM in Bakersfield, the $PM_{2.5}$ data were from the SFS sampler. The regression results in Table 4-4 were obtained using the model in **Equation 4-2**, where it is assumed that the light-scattering efficiencies $E_{2.5}$ and E_c are constant.

$$b_{sp} = A + E_{2.5}\, PM_{2.5} + E_c\, PM_c \qquad \textbf{(4-2)}$$

Both $PM_{2.5}$ and PM_c are strongly influenced by meteorology, and therefore are somewhat collinear. This violates one of the assumptions of the regression model, which is that the independent variables are not correlated. The consequence is that the regression analysis overestimates the importance of the variable that is more accurately measured and underestimates the importance of the variable that is less accurately measured. In this case,

$PM_{2.5}$ is measured directly and PM_c is estimated from the difference of measurements. Therefore, it is a reasonable result that the values of $E_{2.5}$ from Equation 4-2 in Table 4-4 are typically larger than the values from Equation 4-1 in Table 4-2. It is also reasonable that the values of E_c are variable, and sometimes even negative. Negative values for E_c have been observed before (Lowenthal et al., 1995).

There is also a straightforward physical reason for negative values for E_c in regressions based on Equation 4-2, even in the absence of any measurement or regression error. The explanation has been published by White et al. (1994). In the algebra in the remainder of this subsection, the subscript f is used instead of the subscript 2.5 to indicate fine particles, which have a diameter less than 2.5 μm. Then Equation 4-1 becomes

$$b_{sp} = A + E_f\, PM_f + E_c\, PM_c \qquad \textbf{(4-3)}$$

Also, accumulation mode particles will be called smog particles in the remainder of this subsection.

A physical reason for the negative values for E_c in the regression results in Tables 4-4 and 4-6 is that the light-scattering efficiencies E_f and E_c are not constant, as assumed in the regression model. In fact, both vary with the PM composition. The smog fraction of PM_f has a scattering efficiency five or more times larger than the small-particle tail of the dust particle size distribution in the size range below 2.5 μm. Thus, E_f can decrease by a factor of five or more as the PM composition changes from mostly smog particles to mostly dust particles. The regression model accounts for this decrease in E_f, which is a constant in the model, by assigning a negative value to E_c.

White et al. (1994) develop a more appropriate regression model by introducing four light-scattering efficiencies for the fine and coarse particle-size fractions of the smog and dust particles. As long as the size distributions of the smog and dust particles remain constant, the values of these four light-scattering efficiencies will remain constant during variations in the relative amounts of smog and dust. These four efficiencies are identified by subscripts: f and c for fine and coarse, as defined above, and s and d for smog and dust, respectively. Thus E_{df} is the light-scattering efficiency for the portion of the dust particle size distribution in the fine particle-size fraction. White et al. also introduce the fraction of smog in the coarse particle size range F_{sc} and the fraction of dust in the fine particle size range F_{df}. These also remain constant as long as the separate size distributions of the smog and dust particles remain constant.

After some algebraic manipulation and the omission of second order terms, Equation 4-3 can be replaced by

$$b_{sp} \approx [E_{sf} + (E_{sc} - E_{dc})F_{sc}]PM_f\ \ [(E_{df} - E_{sf})F_{df} + E_{dc}]PM_c \qquad \textbf{(4-4)}$$

where the regression coefficients of PM_f and PM_c are constant as long as the size distribution of the smog and dust components of the PM are constant. The coefficients of PM_f and PM_c now remain constant while the relative amounts of smog and dust aerosol vary.

The data presented above indicate that E_{sf} is about 5 m^2/g, while the data in Figure 4-5 indicate that E_{df} can be equal to or less than 1 m^2/g. Also, the measurements of White et al.

(1994) indicate the value of E_{dc} is approximately 0.5 m^2/g. Thus, if the particle size distribution of the dust is such that more than 5 to 10 percent of the dust is in the fine particle size range, the regression coefficient for PM_c in Equation 4-4 will be negative.

The regression coefficient of PM_f in Equation 4-4 is expected to be approximately equal to E_{sf}. The reasons for this are that F_{sc} is expected to be small, and also E_{sc} and E_{dc} are five to ten times smaller than E_{sf}. Thus, the regression coefficient of PM_f obtained from regressions of b_{sp} against both PM_f and PM_c should be similar to the regression coefficient from the regression of b_{sp} against PM_f alone. Because of the lack of chemical species concentrations from collocated filter $PM_{2.5}$ and PM_{10}, it is not possible to determine values for F_{sc} and F_{df} that are needed to perform the calculations suggested by Equation 4-4.

If the smog and/or dust size distributions vary from site to site or season to season, the regression coefficients in Equation 4-4 will have different values for different sites and seasons. It is likely that variations in PM size distributions contribute to the variability of the regression coefficients in Table 4-4.

Table 4-4. Regression results for the dependence of 24-hour b_{sp} on $PM_{2.5}$ and PM_c. The measurement method used to calculate PM_c is indicated.

Category	Site	Intercept Mm^{-1}	Standard Error Mm^{-1}	Slope m^2/g	Standard Error m^2/g	PM_c slope	Standard Error m^2/g	Number of Data Points	R^2	PM Measurement Methods
All Data	Angiola	22.3	8.0	4.90	0.21	-0.73	0.16	242	0.70	$PM_{2.5}$ - SFS, PM_c - BAM
Cool	Angiola	39.3	12.8	5.17	0.31	-1.45	0.51	123	0.71	$PM_{2.5}$ - SFS, PM_c - BAM
Warm	Angiola	15.5	5.9	1.87	0.30	0.02	0.02	119	0.26	$PM_{2.5}$ - SFS, PM_c - BAM
All Data	Bakersfield	10.2	8.2	6.39	0.16	-1.27	0.09	327	0.84	$PM_{2.5}$ - SFS, PM_c - BAM
Cool	Bakersfield	33.6	11.6	6.99	0.24	-2.61	0.42	171	0.86	$PM_{2.5}$ - SFS, PM_c - BAM
Warm	Bakersfield	5.7	8.4	1.80	0.43	0.36	0.19	156	0.18	$PM_{2.5}$ - SFS, PM_c - BAM
All Data	Bakersfield	-19.5	22.5	5.87	0.50	-0.31	0.81	49	0.77	$PM_{2.5}$ - SFS, PM_c - Dichot
Cool	Bakersfield	-14.5	26.2	6.77	0.75	-1.31	1.59	25	0.88	$PM_{2.5}$ - SFS, PM_c - Dichot
Warm	Bakersfield	33.6	26.6	0.41	0.92	0.24	0.74	24	0.02	$PM_{2.5}$ - SFS, PM_c - Dichot
All Data	Bakersfield	-15.9	13.7	6.64	0.25	-0.65	0.55	54	0.95	$PM_{2.5}$ - SFS, PM_c - FRM
Cool	Bakersfield	-3.0	18.5	6.68	0.45	-1.11	1.12	31	0.95	$PM_{2.5}$ - SFS, PM_c - FRM
Warm	Bakersfield	-46.8	31.8	6.45	2.31	0.32	0.72	23	0.33	$PM_{2.5}$ - SFS, PM_c - FRM
All Data	Bakersfield	-16.5	13.4	6.53	0.24	-0.59	0.53	54	0.95	$PM_{2.5}$.5 and PM_c - FRM
All Data	Fresno	26.3	4.4	6.00	0.11	-1.41	0.18	329	0.91	$PM_{2.5}$ - SFS, PM_c - BAM
Cool	Fresno	-4.2	4.4	5.89	0.09	-2.76	0.15	169	0.96	$PM_{2.5}$ - SFS, PM_c - BAM
Warm	Fresno	60.3	6.8	6.35	0.17	-3.87	0.39	160	0.90	$PM_{2.5}$ - SFS, PM_c - BAM
All Data	Fresno	21.8	13.6	6.16	0.23	-1.65	0.69	56	0.93	$PM_{2.5}$ - SFS, PM_c - Dichot

Table 4-4. Regression results for the dependence of 24-hour bsp on PM2.5 and PMc. The measurement method used to calculate PMc is indicated.

Category	Site	Intercept Mm^{-1}	Standard Error Mm^{-1}	Slope m^2/g	Standard Error m^2/g	PM_c slope	Standard Error m^2/g	Number of Data Points	R^2	PM Measurement Methods
Cool	Fresno	41.6	22.9	6.18	0.38	-3.14	1.89	30	0.92	$PM_{2.5}$ - SFS, PM_c - Dichot
Warm	Fresno	-17.5	6.9	8.95	0.62	-1.29	0.36	26	0.91	$PM_{2.5}$ - SFS, PM_c - Dichot
All Data	Fresno	23.2	15.5	5.97	0.24	-1.35	0.73	59	0.92	$PM_{2.5}$ - SFS, PM_c - FRM
Cool	Fresno	33.0	26.0	5.79	0.35	-1.04	1.60	31	0.91	$PM_{2.5}$ - SFS, PM_c - FRM
Warm	Fresno	-7.8	10.8	7.48	0.76	-1.02	0.45	28	0.80	$PM_{2.5}$ - SFS, PM_c - FRM
All Data	Fresno	18.1	16.0	5.03	0.20	-0.61	0.75	59	0.92	$PM_{2.5}$ and PM_c - FRM
Cool	Clovis	-98.9	70.0	5.19	0.77	5.68	1.67	8	0.92	$PM_{2.5}$-MiniVol, PM_c – FRM
Cool	Corcoran	6.5	8.4	7.14	0.29	-0.16	0.11	6	1.00	$PM_{2.5}$-MiniVol, PM_c – BAM
Cool	Corcoran	53.4	23.0	5.05	0.46	-0.45	0.56	9	0.95	$PM_{2.5}$ and PM_c - MiniVol
All Data	Corcoran	86.8	37.4	4.30	0.55	-0.22	1.02	17	0.82	$PM_{2.5}$-MiniVol, PM_c - FRM
Cool	Corcoran	97.4	49.3	3.85	0.67	0.61	1.83	13	0.79	$PM_{2.5}$-MiniVol, PM_c - FRM
Warm	Edwards	20.1	7.2	0.06	1.29	0.01	0.24	7	0.00	$PM_{2.5}$ -MiniVol, PM_c - BAM
Cool	Modesto	4.2	30.2	5.59	0.80	-1.24	3.96	6	0.98	$PM_{2.5}$-MiniVol, PM_c - Dichot
Cool	Modesto	5.0	21.3	4.87	0.26	0.48	1.72	13	0.98	$PM_{2.5}$ -MiniVol, PM_c - FRM
Cool	Oildale	77.5	55.3	4.89	0.65	-3.79	2.85	10	0.90	$PM_{2.5}$ -MiniVol, PM_c - FRM
Cool	Stockton	113.4	198.5	-0.22	8.53	6.01	15.97	5	0.14	$PM_{2.5}$ - MiniVol, PM_c - Dichot
Cool	Stockton	-54.9	47.2	4.70	1.14	3.98	2.26	10	0.87	$PM_{2.5}$ -MiniVol, PM_c - FRM
Cool	Visalia	89.6	55.3	4.89	0.69	-1.45	2.10	11	0.87	$PM_{2.5}$ -MiniVol, PM_c - FRM

4.3 DEPENDENCE ON RELATIVE HUMIDITY

Figure 4-6 shows the light-scattering efficiency calculated by dividing hourly b_{sp} by hourly BAM $PM_{2.5}$ as a function of the RH measured in the RR nephelometer at Bakersfield. Hourly data were used to avoid the wide variations in RH that occur during filter measurement periods. To minimize the effects of measurement errors, only cool season data with $PM_{2.5}$ greater than 10 $\mu g/m^3$ are included. The majority of variability in scattering efficiencies occurs when the RH is greater than 65%. The scattering efficiency as a function of RH for data with RH less than or equal to 65% is

$$\text{Scattering Efficiency} = (3.82 \pm 0.10)\ m^2/g + (0.022 \pm 0.002)\ m^2/(g\ \%) * RH \qquad \textbf{(4-5)}$$

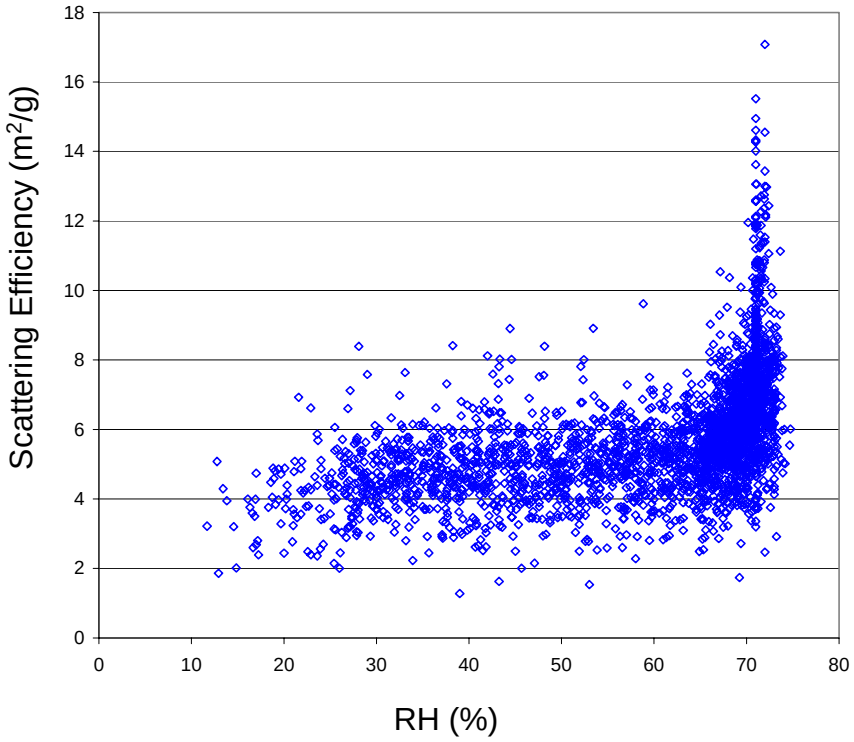

Figure 4-6. November through April hourly light-scattering efficiencies versus RH in the RR nephelometer at Bakersfield.

Similar results were found at Angiola and are shown in **Figure 4-7**. These data are restricted to $PM_{2.5}$ greater than 10 $\mu g/m^3$ and to December 13, 2000 through February 2, 2001 to match the time period when liquid water content (LWC) data are available. The scattering efficiency as a function of RH for cool season data with RH less than or equal to 65% is

$$\text{Scattering Efficiency} = (2.00 \pm 0.19)\ m^2/g + (0.060 \pm 0.004)\ m^2/(g\ \%) * RH \qquad \textbf{(4-6)}$$

Of the 22 points with scattering efficiencies greater than 15 m^2/g, 13 were measured during fog episodes that had a LWC greater than 100 mg/m^3. However, some light-scattering efficiencies measured during fog events were close to, or below the regression line in Equation 4-2. These data are shown by the open symbols in Figure 4-7. The majority of the high light-scattering efficiencies were measured during fog events, but not all efficiencies measured during fog events were high.

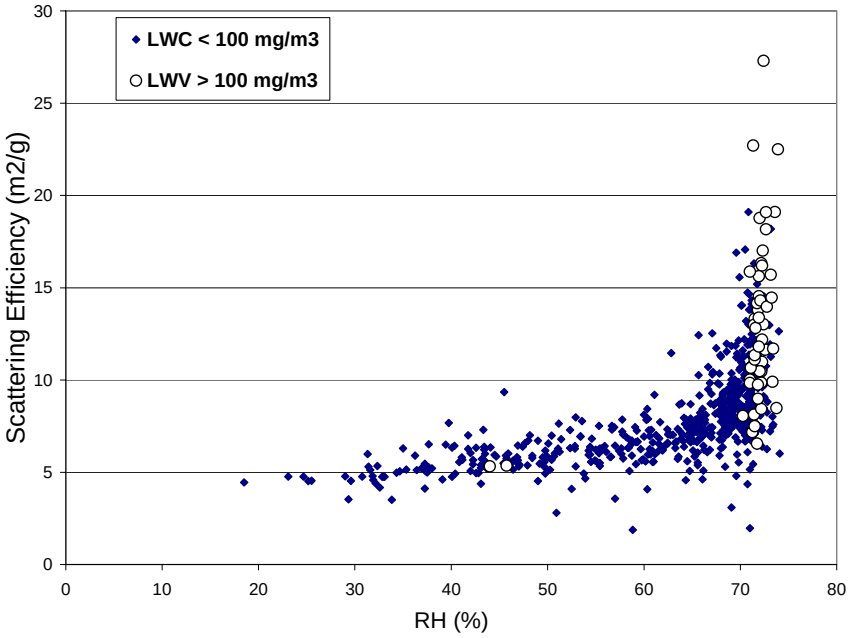

Figure 4-7. December 13, 2000 through February 2, 2001 hourly light-scattering efficiencies versus RH in the RR nephelometer at Angiola. Points measured when LWC ≥ 100 mg/m^3 are shown by open circles.

Figure 4-8 shows scatter plots of hourly b_{sp} data versus BAM $PM_{2.5}$ at Angiola and Bakersfield stratified by sampling chamber RH. Two RH strata used are less than or equal to 65% and greater than 65%. Only cool season data are shown. There is more scatter in the b_{sp} to BAM $PM_{2.5}$ relationship when the sampling chamber RH is greater than 65%. **Table 4-5** presents the relationships between hourly b_{sp} and BAM $PM_{2.5}$ for Angiola and Bakersfield in the cool season. Both the relationships using data taken under all sampling chamber RH conditions and data collected when the sampling chamber RH is less than or equal to 65% are shown.

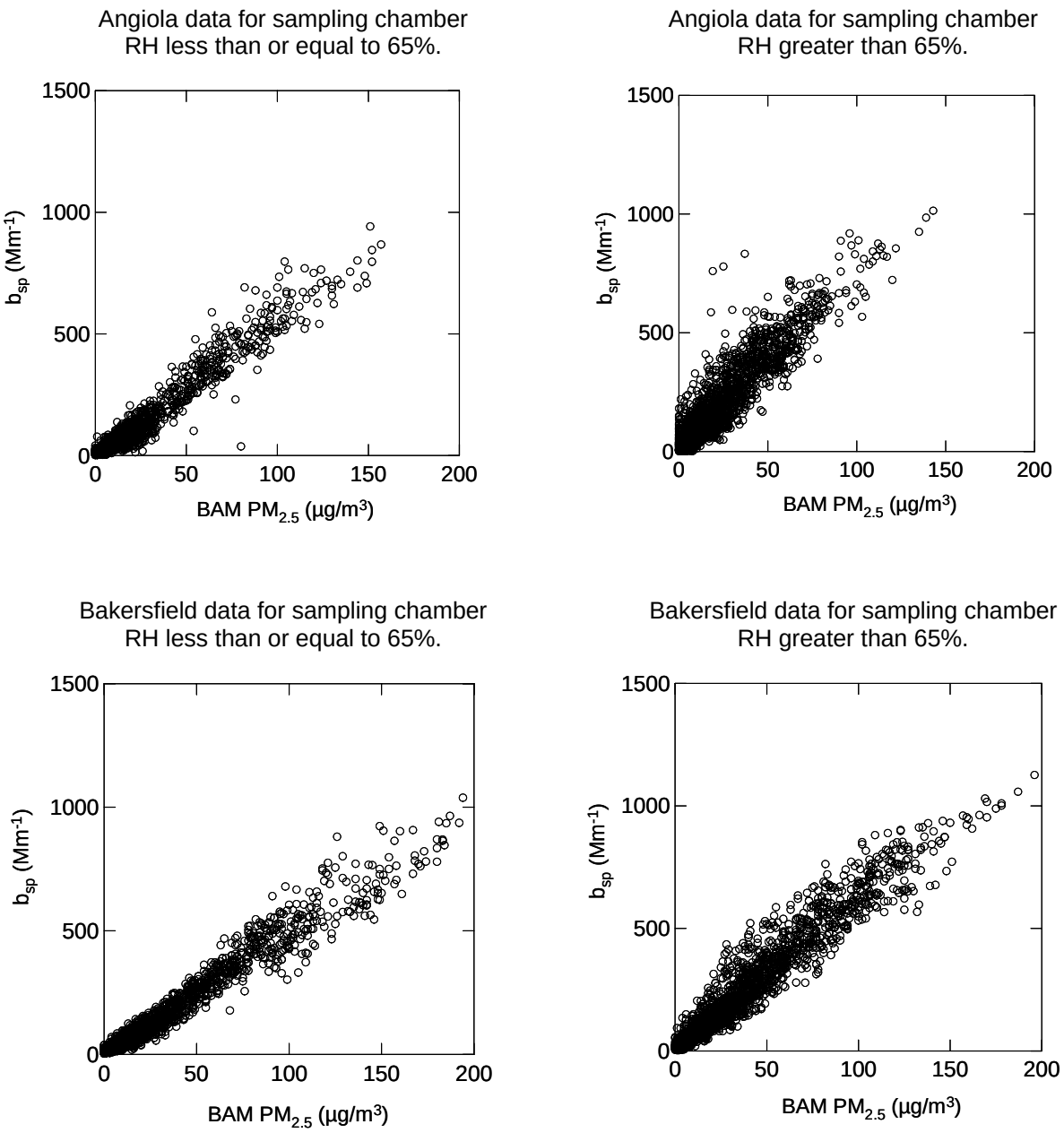

Figure 4-8. Cool season hourly b_{sp} versus BAM $PM_{2.5}$ at Angiola and Bakersfield stratified by RH in the RR nephelometer.

Table 4-5. Regression results for comparison between hourly b_{sp} and BAM $PM_{2.5}$ for cool season data at Angiola and Bakersfield. Only hours with BAM $PM_{2.5}$ greater than 10 $\mu g/m^3$ were included.

Site	RH (%)	Intercept (Mm^{-1})		Slope (m^2/g)		Number of Data Points	R^2
		Value	Standard Error	Value	Standard Error		
Angiola	All Data	16.6	3.3	6.54	0.07	2277	0.79
		0.0	Forced	6.83	0.04	2277	0.79
	RH ≤ 65%	-26.4	2.7	6.00	0.05	924	0.93
		0.0	Forced	5.60	0.04	924	0.92
	RH > 65%	28.5	4.2	7.42	0.10	1353	0.81
		0.0	Forced	7.97	0.05	1353	0.81
Bakersfield	All Data	11.8	2.2	5.54	0.04	2956	0.89
		0.0	Forced	5.69	0.02	2956	0.89
	RH ≤ 65%	-2.2	1.9	5.01	0.03	1442	0.95
		0.0	Forced	4.98	0.02	1442	0.95
	RH > 65%	23.6	3.1	6.05	0.05	1514	0.91
		0.0	Forced	6.36	0.03	1514	0.91

Table 4-6 shows the multiple variable regression of b_{sp} versus $PM_{2.5}$ and PM_c stratified by RH. The scattering efficiencies from the b_{sp} to $PM_{2.5}$ regressions are not significantly different than the fine particle scattering efficiencies from the b_{sp} to $PM_{2.5}$ and PM_c regressions. For example, the scattering efficiency as calculated from the b_{sp} data and BAM $PM_{2.5}$ at Bakersfield is 4.9 m^2/g and the fine particle scattering efficiency is 4.9 m^2/g. The fine particle scattering efficiencies and the regression intercepts, from both the single variable and multi-variable regressions, are smaller in the lower RH range.

Table 4-6. Regression results for the dependence of hourly b_{sp} on BAM $PM_{2.5}$ and PM_c for the cool season at Angiola and Bakersfield. Results for all data and RH ≤ 65% are shown.

Site	Intercept (Mm^{-1})	$PM_{2.5}$ Slope (m^2/g)	PMc Slope (m^2/g)	N	R^2	Category
Angiola	18.0	6.46	-0.17	3575	0.83	All RH values
Angiola	-3.5	5.64	-0.19	1455	0.94	RH ≤ 65%
Bakersfield	15.5	5.64	-0.29	4019	0.92	All RH values
Bakersfield	6.6	4.94	-0.13	2114	0.96	RH ≤ 65%

5. RECOMMENDATIONS

It is recommended that the b_{sp} data measured during the cool season in the SJV be used to estimate $PM_{2.5}$. During this season, the b_{sp} data meet the objective set for them in the program plan of greatly increasing the time and spatial resolution of estimates of the $PM_{2.5}$.

During the cool season (November through April), when the contribution of dust to the PM concentrations is small, the recommended light-scattering efficiency for estimating $PM_{2.5}$ from b_{sp} varies linearly from approximately 4.0 m^2/g when the RH in the nephelometer is 20% to about 5.7 m^2/g at 70% RH. For individual readings, the standard error in the light-scattering efficiency is roughly 1 m^2/g. These values are an average of the values predicted by the regression results in Equations 4-5 and 4-6.

For model evaluation or more detailed analyses, it is recommended that the site-specific cool season light-scattering efficiencies (regression slopes) in Table 4-2 be used. It should be recognized that these are empirical regression results that enable estimating $PM_{2.5}$ from b_{sp} measurements that respond to both fine and coarse particle sizes.

For most analyses, it is recommended that b_{sp} measurements during the warm season be used as a semi-quantitative indicator of PM concentrations. The exception is events in the desert where fire smoke or smog has transported into the desert at relatively high concentrations. At these times, the b_{sp} measurements in the desert provide a useful indicator of $PM_{2.5}$.

When evaluating and validating computer models that separately estimate the $PM_{2.5}$ and PM_c, the warm season data become more useful. In this case, it is possible to assign separate light scattering efficiencies to the two size fractions and calculate a simulated value for b_{sp} to be compared with the measured data.

It is recommended that before RR nephelometers are again used in a similar field study, tests be performed to better understand the anomalously high b_{sp} readings sometimes observed when the RH in the nephelometer is near 70%. Hypotheses to be explored should include the possibility that the residence time of the sample air flow between the heater and the nephelometer scattering chamber was inadequate to dry the PM. Setting the RH threshold of the smart heater to a lower value may not solve this problem. It may only move the RH range where the anomalously high b_{sp} readings are observed to a lower value, so more of the data are included in this range.

This page is intentionally blank.

6. REFERENCES

Hafner H.R., Hyslop N.P., and Green C.N. (2003) California Regional $PM_{10}/PM_{2.5}$ Air Quality Study management of anchor site data. Prepared for the San Joaquin Valleywide Air Pollution Study Agency and the California Air Resources Board, Sacramento, CA, by Sonoma Technology, Inc., Petaluma, CA, 999242-2087-FR, May. Available on the Internet at <http://www.arb.ca.gov/airways/Documents/preliminary/STI/STIDMFR.pdf> last accessed November 22, 2004.

Hyslop N.P., Brown S.G., Gorin C.A., and Hafner H.R. (2003) California Regional $PM_{10}/PM_{2.5}$ Air Quality Study (CRPAQS) data quality summary reports. Final report prepared for San Joaquin Valleywide Air Pollution Study Agency c/o California Air Resources Board, Sacramento, CA, by Sonoma Technology, Inc., Petaluma, CA, STI-999242-2310-FR, February. Available on the Internet at <http://www.arb.ca.gov/airways/Documents/preliminary/STI/STIDQSR.pdf> last accessed November 22, 2004.

Lowenthal D.H., Rogers C.F., Saxena P., Watson J.G., and Chow J.C. (1995) Sensitivity of estimated light extinction coefficients to model assumptions and measurement errors. *Atmos. Environ.* **29**, 751-766.

Richards L.W., Alcorn S.H., McDade C., Couture T., Lowenthal D., Chow J.C., and Watson J.G. (1999) Optical properties of the San Joaquin Valley aerosol collected during the 1995 Integrated Monitoring Study. *Atmos. Environ.* **33**, 4787-4795 (STI-1834).

Richards L.W., Weiss R.E., and Waggoner A.P. (2001) Radiance Research Model 903 integrating nephelometer. In proceedings from *Regional Haze and Global Balance - Aerosol Measurements and Models: Closure, Reconciliation and Evaluation*, S.F. Archer, J.M. Prospero, and J. Core, eds., Air and Waste Management Association, Pittsburgh, PA (STI-2099).

Richards L.W. (2002a) Analysis of data from the collocated operation of four Radiance Research nephelometers at Angiola after the end of the CRPAQS field study. Report prepared for The San Joaquin Valleywide Air Pollution Study Agency c/o California Air Resources Board, Sacramento, CA, by Sonoma Technology, Inc., Petaluma, CA, STI-999213-2292, December (revised). Available on the Internet at <http://www.arb.ca.gov/airways/Documents/preliminary/STI/AppA2DAR.pdf> last accessed November 22, 2004.

Richards L.W. (2002b) Standard operating procedure for radiance research M903 integrating nephelometer. Appendix A.2 of the field operations and quality integrated work plans. Report prepared for The San Joaquin Valleywide Air Pollution Study Agency c/o California Air Resources Board, Sacramento, CA, by Sonoma Technology, Inc., Petaluma, CA, STI-999213, December. Available on the Internet at <http://www.arb.ca.gov/airways/Documents/preliminary/STI/AppA2.pdf> last accessed November 22, 2004.

Technical and Business Systems, Inc. and Parsons Engineering Science, Inc. (2002) Satellite network operations for the California Regional PM_{10} /$PM_{2.5}$ Air Quality Study (CRPAQS). Draft final report prepared for the San Joaquin Valleywide Study Agency and California Air Resources Board by Technical and Business Systems, Inc., Santa Rosa, CA, and Parsons Engineering Science, Inc., Pasadena, CA, June. Available on the Internet at <http://www.arb.ca.gov/airways/Documents/preliminary/T&B/TBDraftFinalReport.pdf> last accessed November 22, 2004.

Watson J.G., DuBois D.W., DeMandel R., Kaduwela A., Magliano K., McDade C., Mueller P.K., Ranzieri A., Roth P.M., and Tanrikulu S. (1998) Aerometric monitoring program plan for the California Regional $PM_{2.5}$/PM_{10} Air Quality Study. Draft report prepared for the California Regional PM_{10}/$PM_{2.5}$ Air Quality Study Technical Committee, California Air Resources Board, Sacramento, CA, by Desert Research Institute, Reno, NV, DRI Document No. 9801.1D5, December.

Watson J.G. (2002) Visibility: Science and regulation. *J. Air & Waste Manag. Assoc.* **52** (6), 628-713.

White W.H., Macias E.S., Nininger R.C., and Schorran D. (1994) Size-resolved measurements of light scattering by ambient particles in the southwestern U.S.A. *Atmos. Environ.* **28**, 909-921.

Wittig A.E., Blumenthal D.L., Roberts P.T., and Hyslop N.P. (2003) California Regional PM_{10}/$PM_{2.5}$ Air Quality Study (CRPAQS) anchor site measurements and operations. Final report prepared for the San Joaquin Valleywide Air Pollution Study Agency c/o California Air Resources Board, Sacramento, CA, by Sonoma Technology, Inc., Petaluma, CA, STI-999231-2332-FR, May. Available on the Internet at <http://www.arb.ca.gov/airways/Documents/preliminary/STI/STIFOFR.pdf> last accessed November 22, 3004.

APPENDIX A

SITE SPECIFIC RELATIONS BETWEEN b_{sp} AND $PM_{2.5}$

This page is intentionally blank.

Figures A-1 and A-2 show scatterplots by site and season of the CRPAQS nephelometer 24-hr average b_{sp} to the SFS and MiniVol $PM_{2.5}$ mass concentrations, respectively. Table A-1 lists the regression results for these scatterplots.

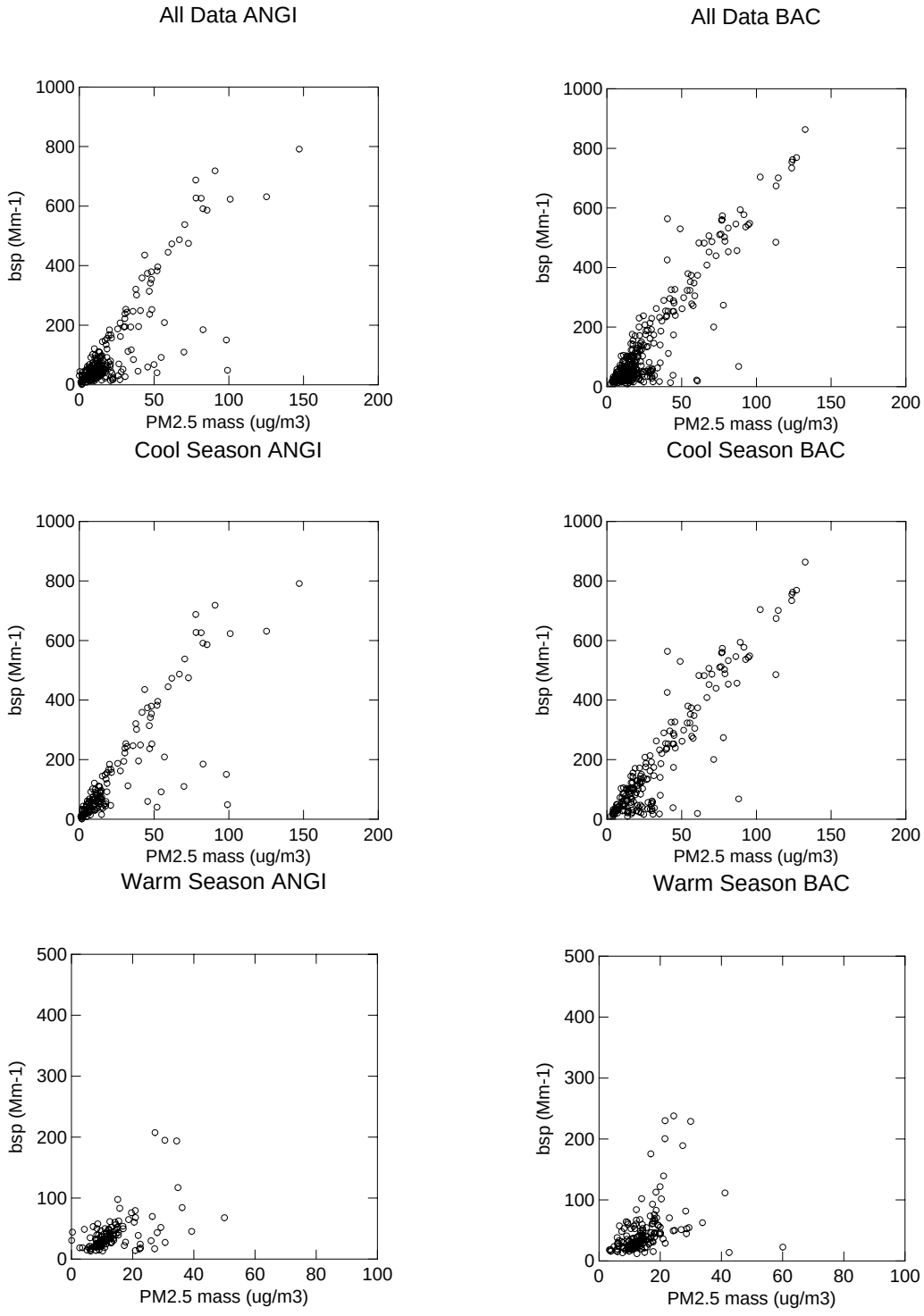

Figure A-1. Scatter plots by site and season of the CRPAQS nephelometer 24-hr average bsp and SFS $PM_{2.5}$ mass concentrations data (page 1 of 2).

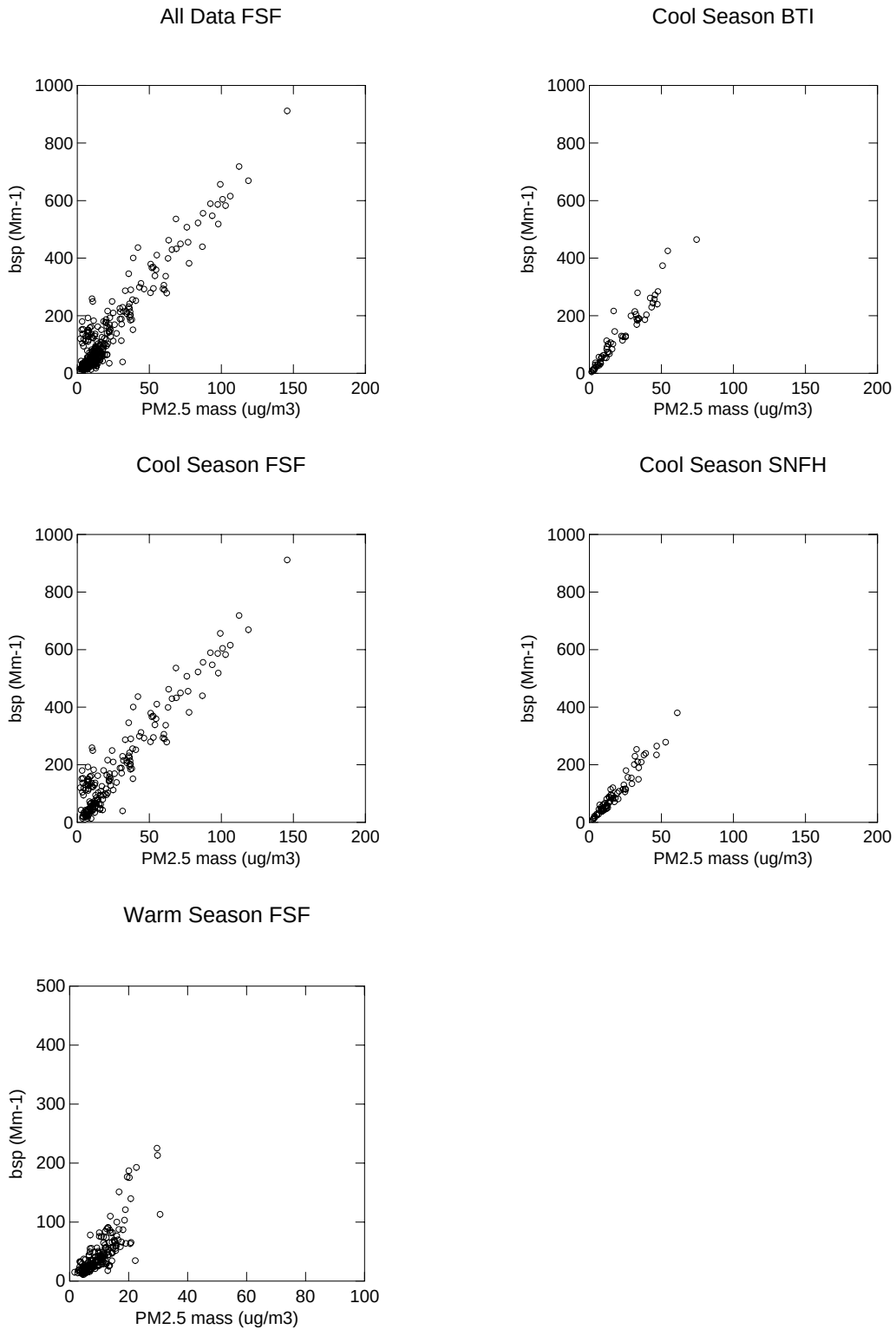

Figure A-1. Scatter plots by site and season of the CRPAQS nephelometer 24-hr average bsp and SFS $PM_{2.5}$ mass concentrations data (page 2 of 2).

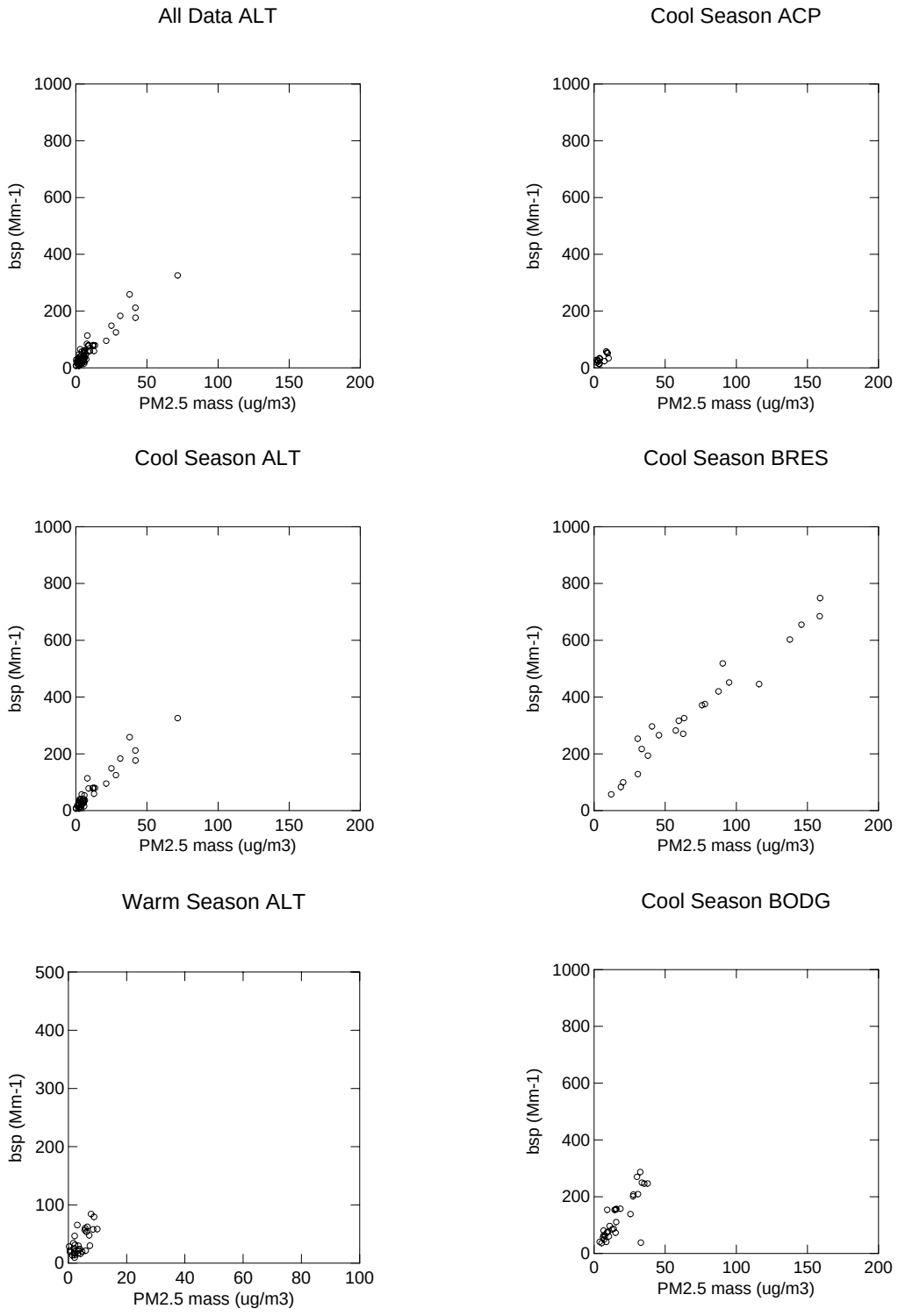

Figure A-2. Scatter plots by site and season of the CRPAQS nephelometer 24-hr average b_{sp} and MiniVol $PM_{2.5}$ mass concentrations data (page 1 of 11).

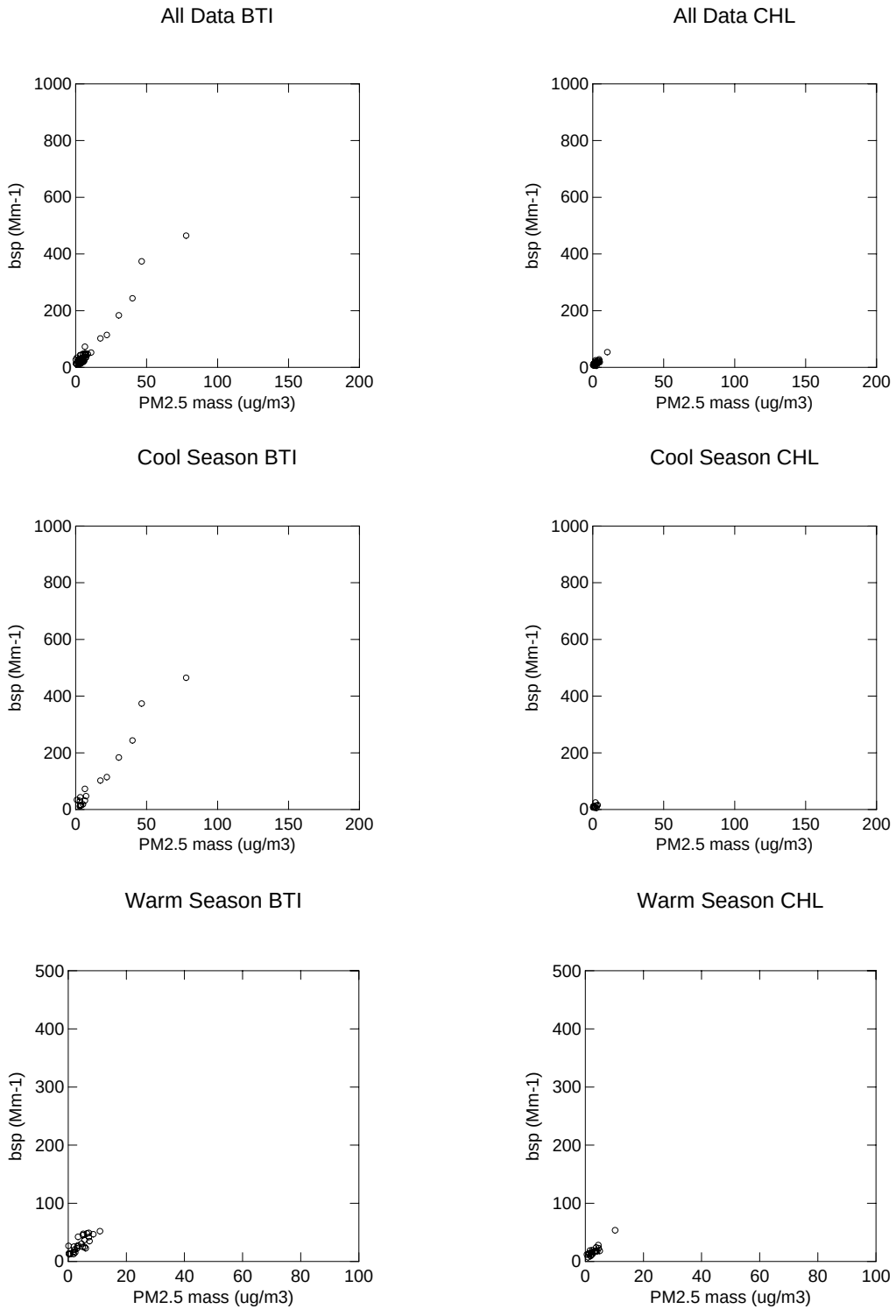

Figure A-2. Scatter plots by site and season of the CRPAQS nephelometer 24-hr average b_{sp} and MiniVol $PM_{2.5}$ mass concentrations data (page 2 of 11).

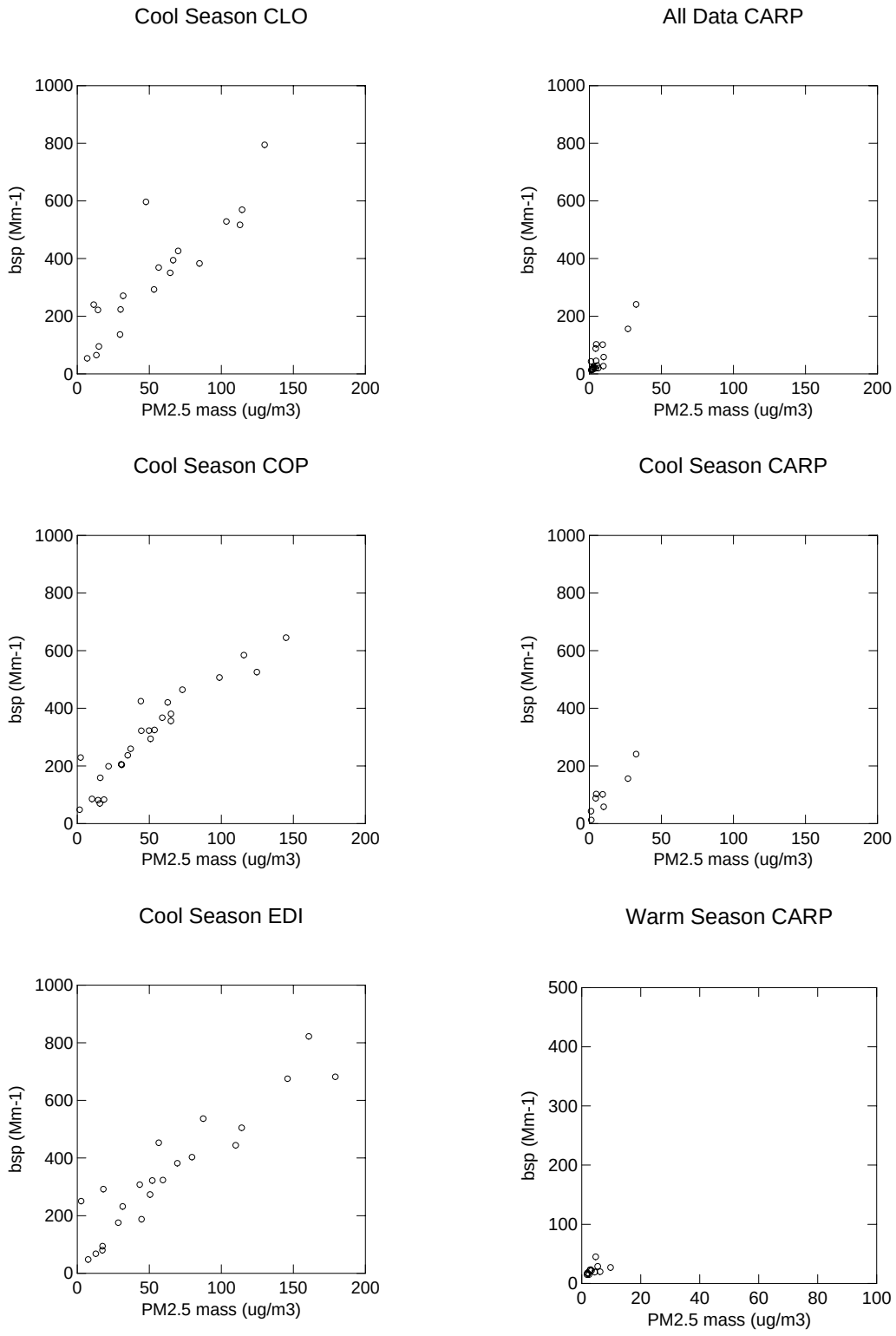

Figure A-2. Scatter plots by site and season of the CRPAQS nephelometer 24-hr average b_{sp} and MiniVol $PM_{2.5}$ mass concentrations data (page 3 of 11).

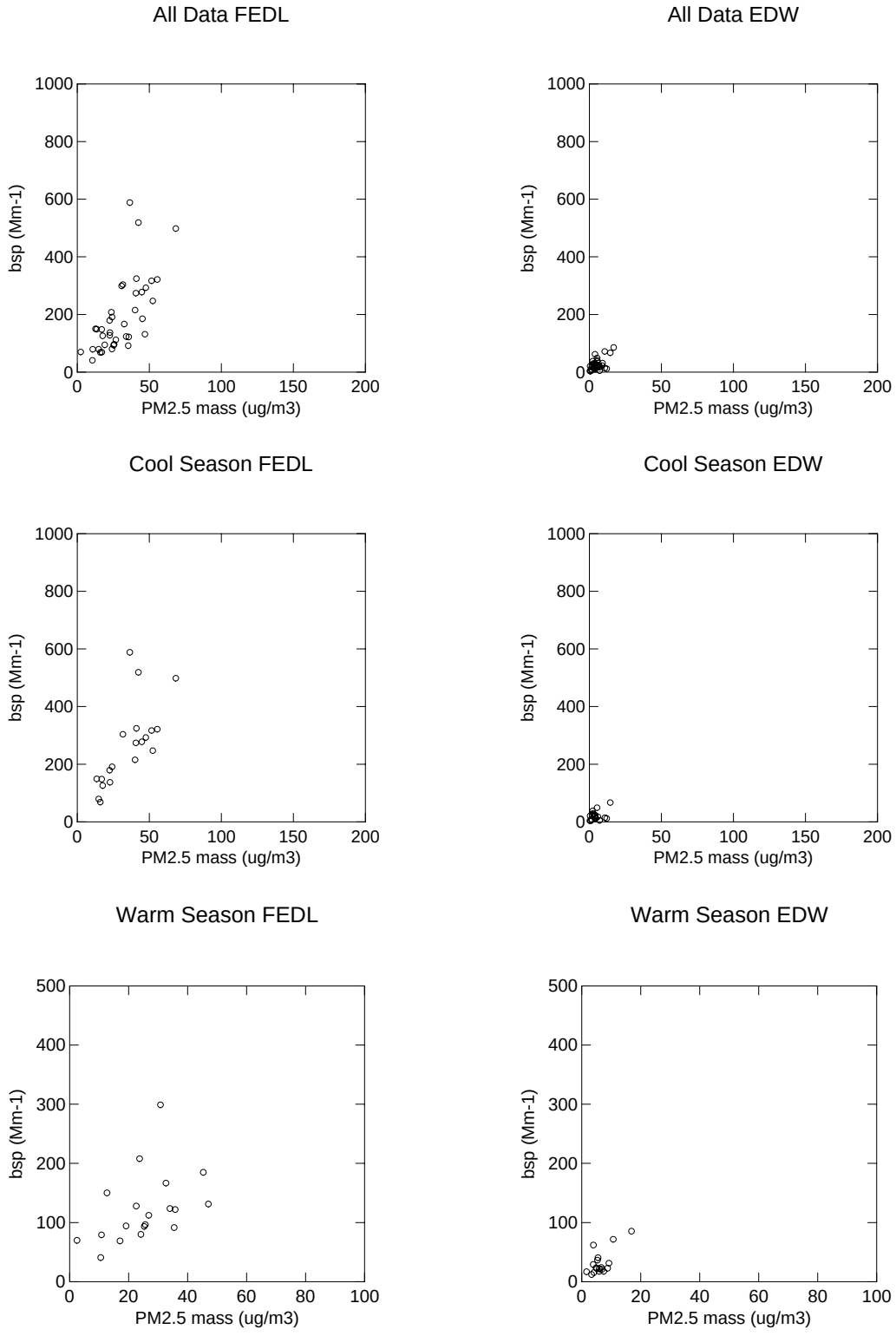

Figure A-2. Scatter plots by site and season of the CRPAQS nephelometer 24-hr average b_{sp} and MiniVol $PM_{2.5}$ mass concentrations data (page 4 of 11).

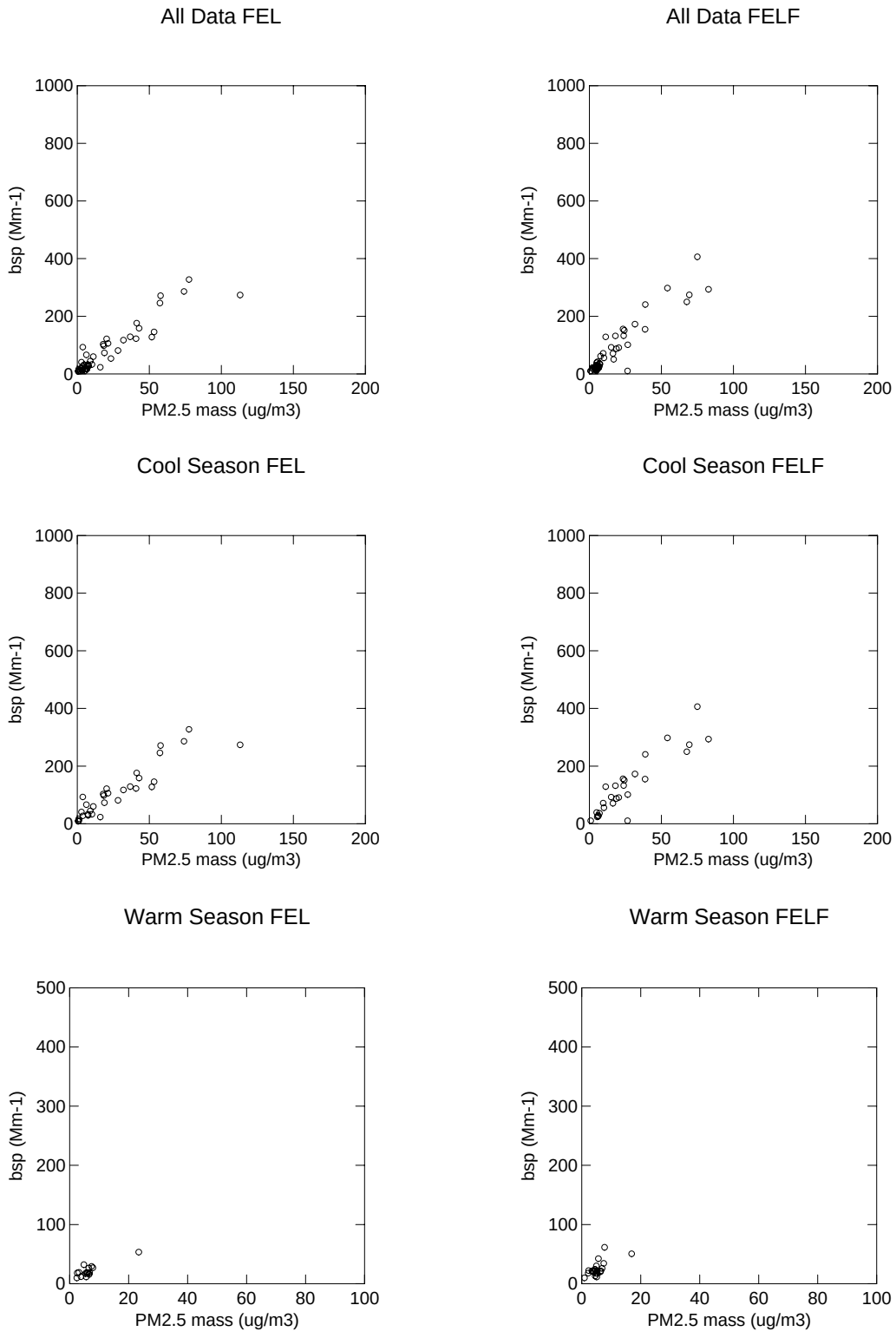

Figure A-2. Scatter plots by site and season of the CRPAQS nephelometer 24-hr average b_{sp} and MiniVol $PM_{2.5}$ mass concentrations data (page 5 of 11).

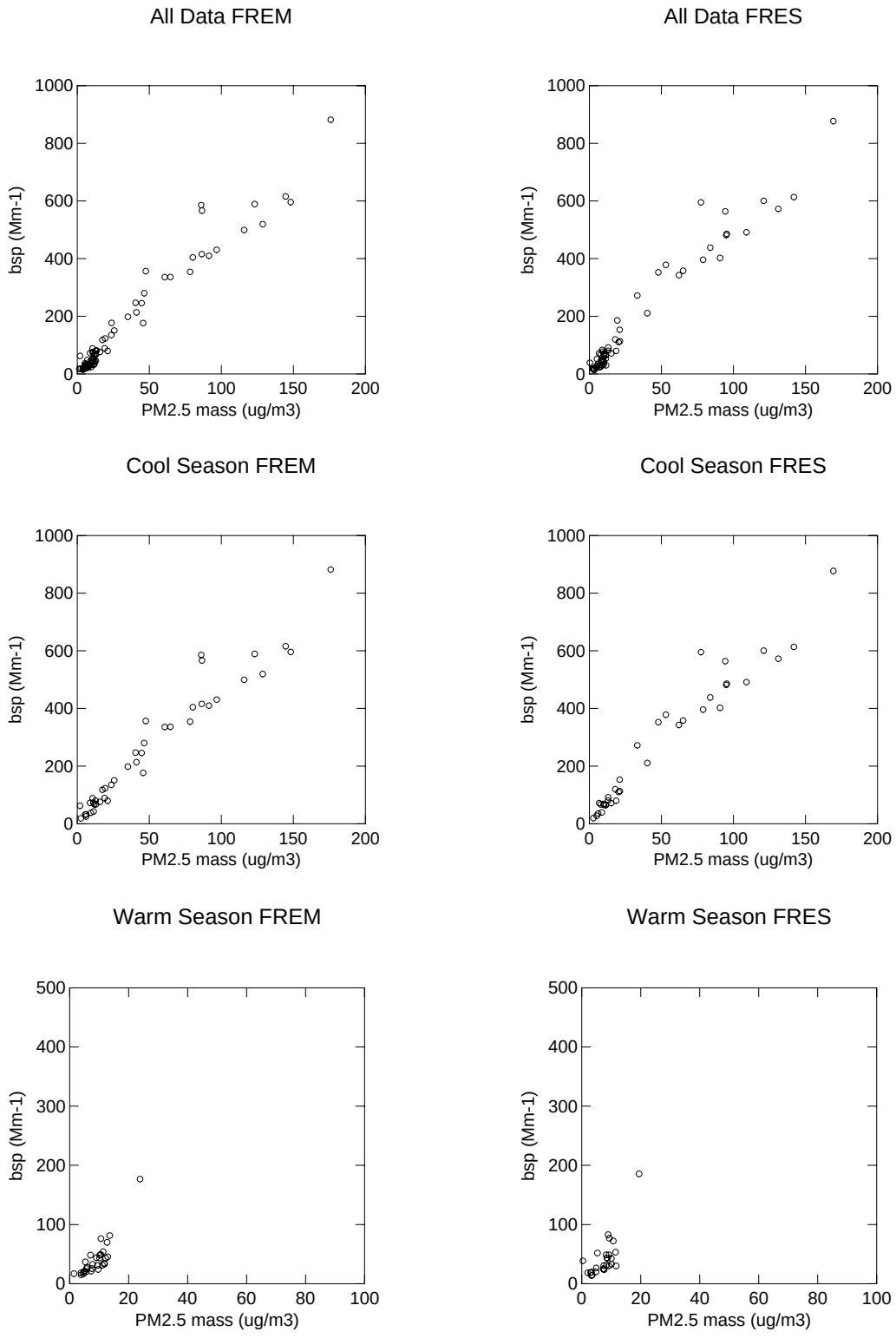

Figure A-2. Scatter plots by site and season of the CRPAQS nephelometer 24-hr average b_{sp} and MiniVol $PM_{2.5}$ mass concentrations data (page 6 of 11).

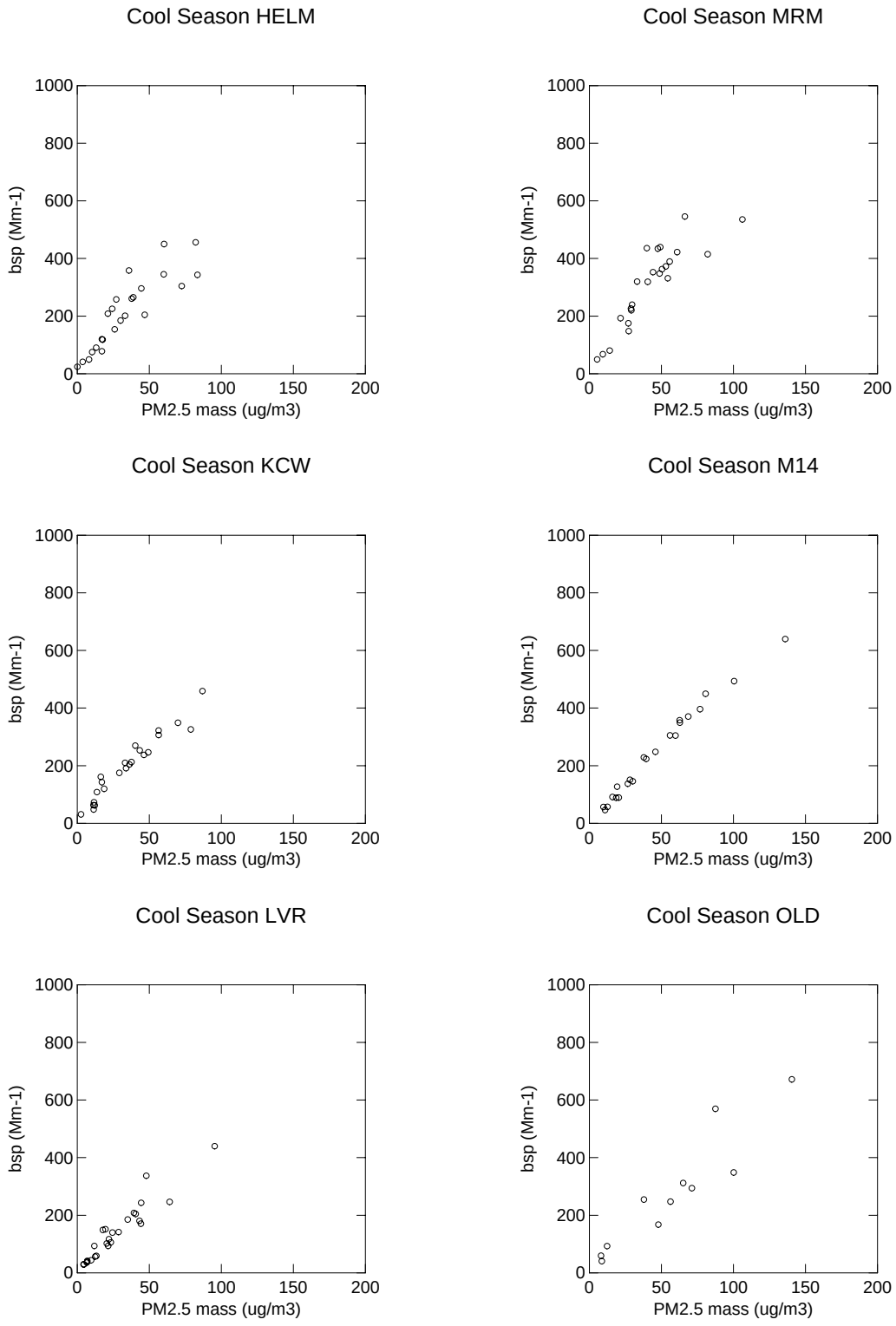

Figure A-2. Scatter plots by site and season of the CRPAQS nephelometer 24-hr average b_{sp} and MiniVol $PM_{2.5}$ mass concentrations data (page 7 of 11).

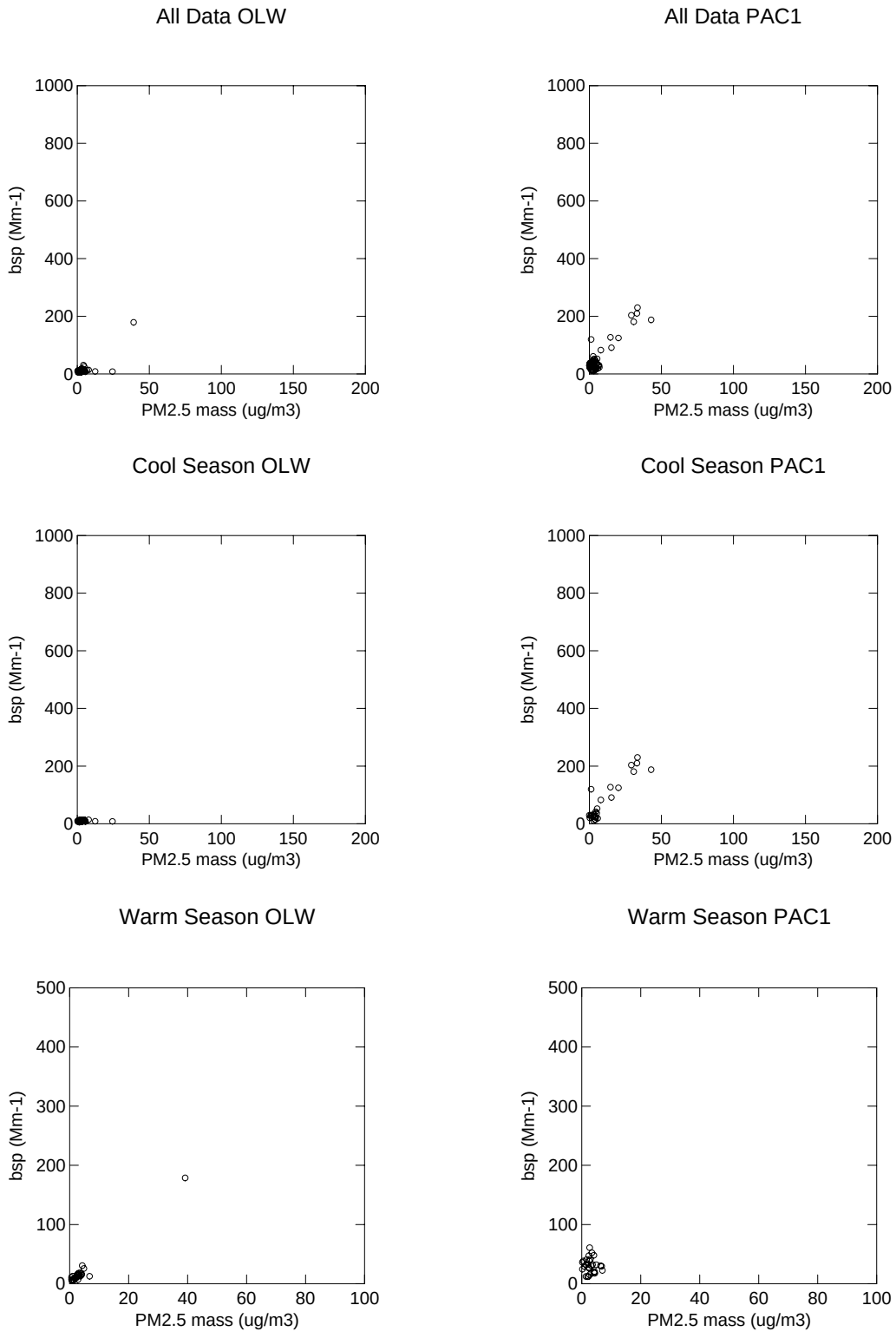

Figure A-2. Scatter plots by site and season of the CRPAQS nephelometer 24-hr average b_{sp} and MiniVol $PM_{2.5}$ mass concentrations data (page 8 of 11).

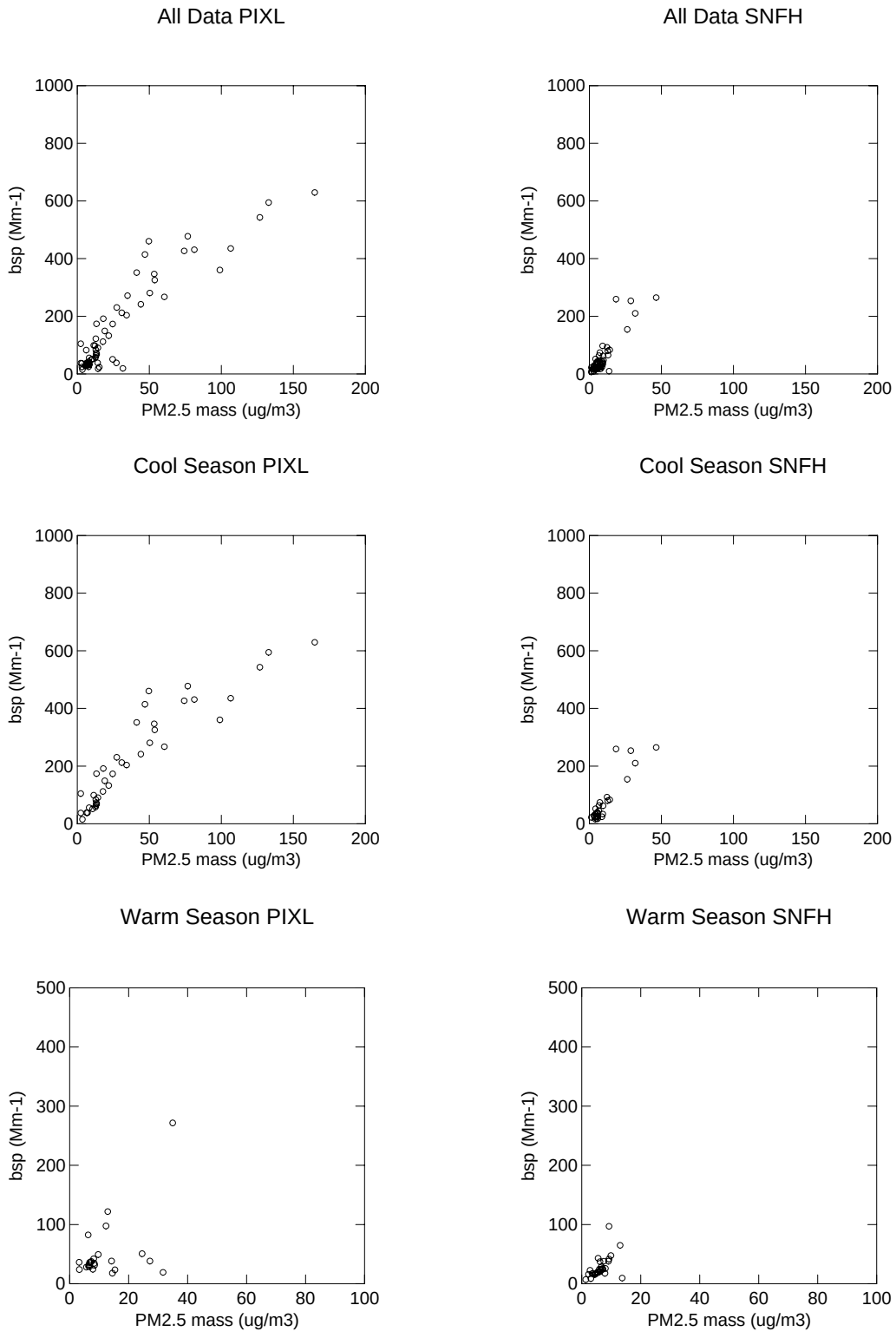

Figure A-2. Scatter plots by site and season of the CRPAQS nephelometer 24-hr average b_{sp} and MiniVol $PM_{2.5}$ mass concentrations data (page 9 of 11).

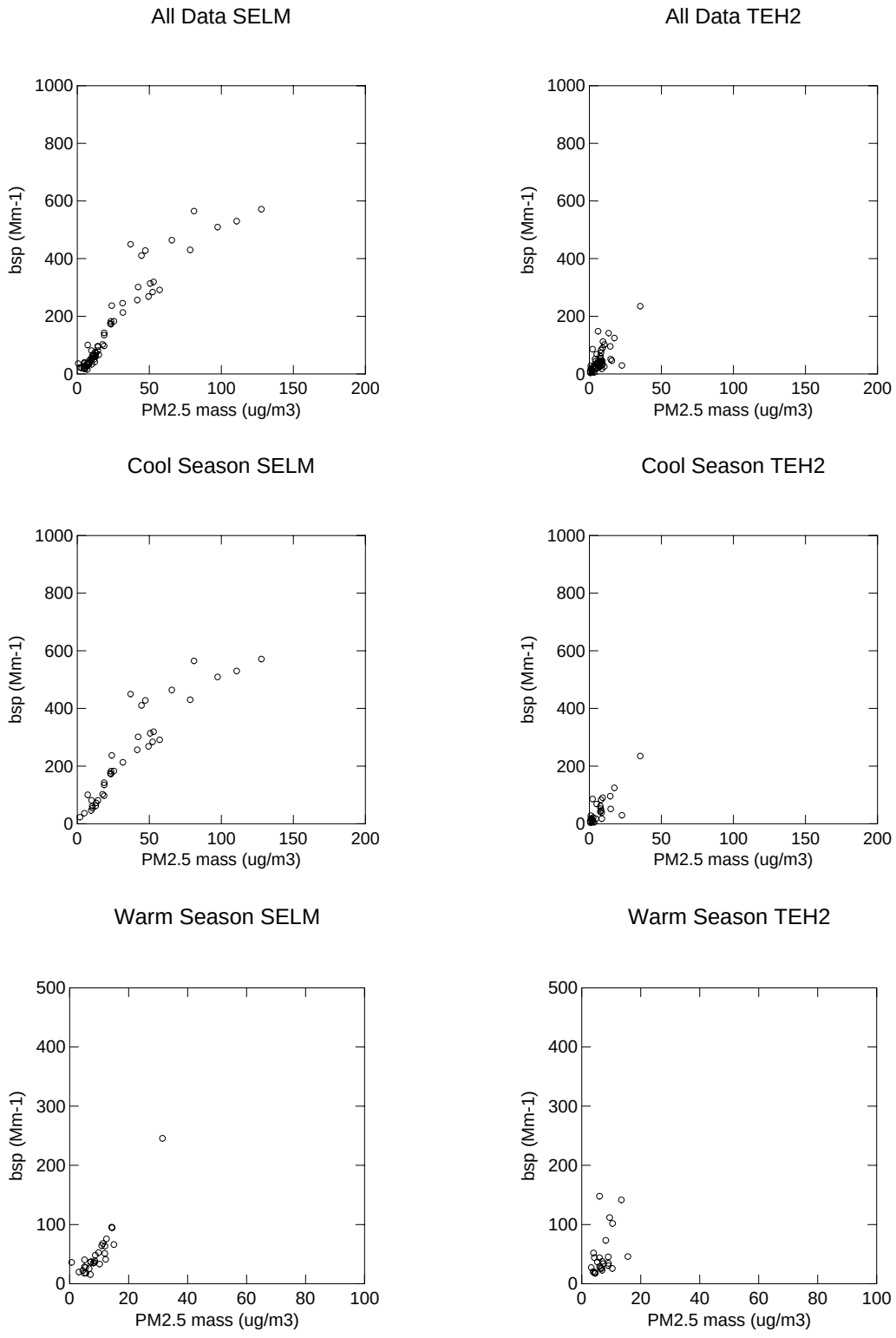

Figure A-2. Scatter plots by site and season of the CRPAQS nephelometer 24-hr average b_{sp} and MiniVol $PM_{2.5}$ mass concentrations data (page 10 of 11).

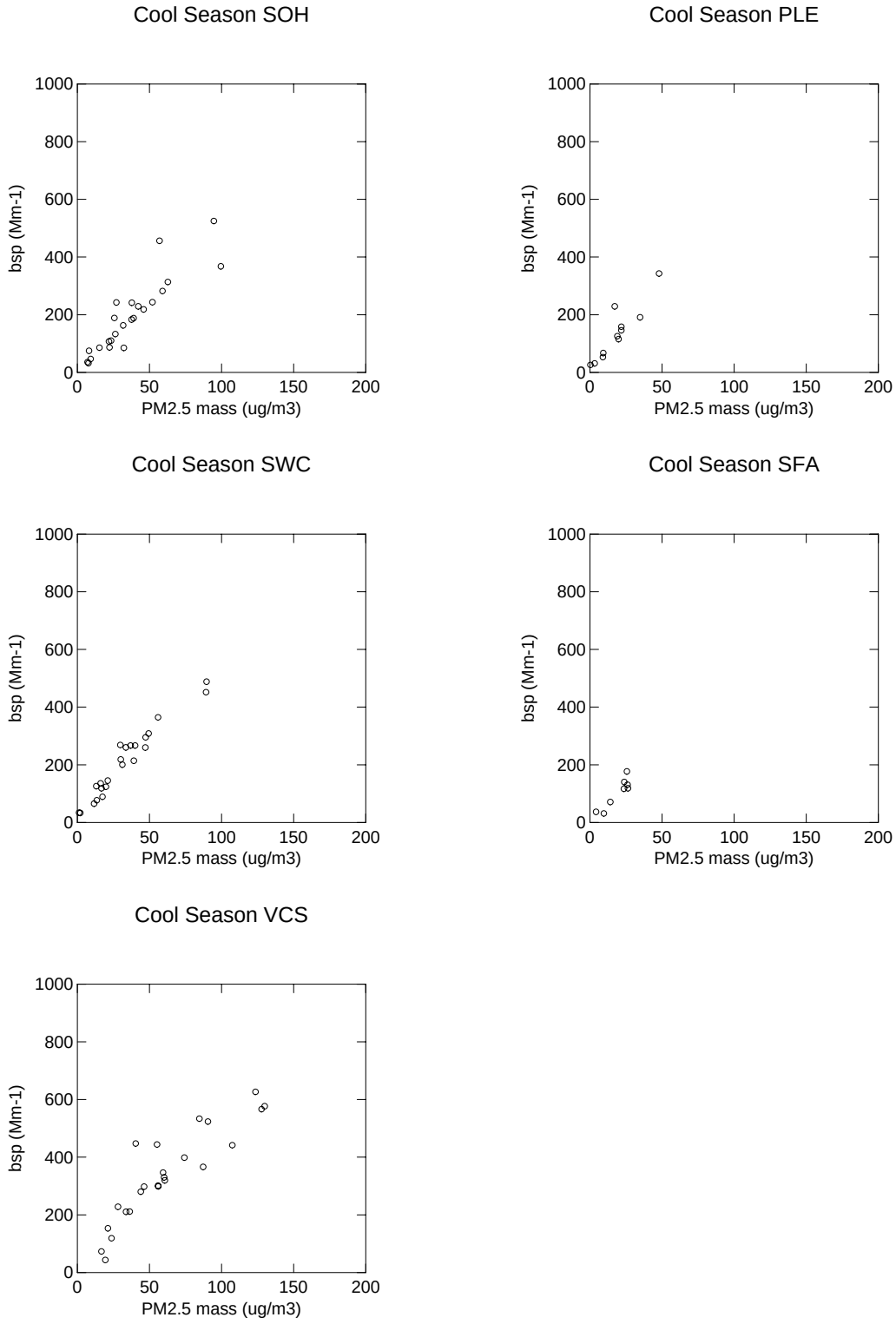

Figure A-2. Scatter plots by site and season of the CRPAQS nephelometer 24-hr average b_{sp} and MiniVol $PM_{2.5}$ mass concentrations data (page 11 of 11).

Table A-1. Regression results for the dependence of 24-hour b_{sp} on filter $PM_{2.5}$ stratified by site for all data from that site and for data stratified by season.

Category	Site	Intercept	$PM_{2.5}$ Slope	Number of Data Points	R^2
All Data	Angiola	-9.7	5.47	255	0.71
Cool	Angiola	12.9	5.39	139	0.72
Warm	Angiola	13.2	2.05	116	0.28
All Data	Bakersfield	-30.7	6.13	349	0.84
Cool	Bakersfield	19.7	6.10	192	0.84
Warm	Bakersfield	15.8	2.14	157	0.16
All Data	Fresno	1.9	6.03	340	0.90
Cool	Fresno	30.1	5.65	169	0.89
Warm	Fresno	-11.4	5.72	171	0.63
Cool	Bethel Island	-1.1	6.13	59	0.92
Cool	Sierra Foothills	-6.1	5.86	64	0.94
All Data	Altamont Pass	15.0	4.66	68	0.90
Cool	Altamont Pass	13.5	4.69	38	0.92
Warm	Altamont Pass	13.3	5.43	30	0.48
Cool	Angels Camp	13.5	3.35	13	0.51
Cool	Bakersfield Res	50.5	4.16	23	0.95
All Data	Bethel Island	3.8	6.21	43	0.96
Cool	Bethel Island	3.1	6.27	17	0.96
Warm	Bethel Island	13.9	3.77	26	0.64
All Data	Bodega Bay	24.3	5.96	32	0.67
Cool	Bodega Bay	24.3	5.96	31	0.66
All Data	China Lake	5.2	4.05	35	0.76
Cool	China Lake	7.7	1.99	14	0.15
Warm	China Lake	5.1	4.20	21	0.84
Cool	Clovis	93.1	4.49	19	0.78
All Data	Corcoran	81.9	4.29	30	0.88
Cool	Corcoran	96.3	4.11	26	0.87
All Data	Carrizo Plain	9.5	6.33	20	0.80
Cool	Carrizo Plain	37.8	5.50	8	0.83
Warm	Carrizo Plain	16.1	1.58	12	0.20
All Data	Dairy Feedlot	12.7	5.98	39	0.46
Cool	Dairy Feedlot	41.4	6.30	20	0.49
Warm	Dairy Feedlot	65.5	2.26	19	0.20
Cool	Edison	101.7	3.82	22	0.86
All Data	Edwards	10.6	2.80	36	0.31
Cool	Edwards	13.6	1.57	18	0.15
Warm	Edwards	5.1	4.09	18	0.46

Table A-1. Regression results for the dependence of 24-hour b_{sp} on filter $PM_{2.5}$ stratified by site for all data from that site and for data stratified by season.

Category	Site	Intercept	$PM_{2.5}$ Slope	Number of Data Points	R^2
All Data	Fellows	13.5	3.17	48	0.86
Cool	Fellows	24.6	3.00	32	0.84
Warm	Fellows	9.2	1.88	16	0.73
All Data	Fellows Fthls	8.8	4.27	49	0.88
Cool	Fellows Fthls	20.2	4.06	27	0.83
Warm	Fellows Fthls	10.3	2.71	22	0.45
All Data	Fresno Motor Vhcl	10.8	4.67	72	0.95
Cool	Fresno Motor Vhcl	27.9	4.49	42	0.94
Warm	Fresno Motor Vhcl	-14.7	6.21	30	0.74
All Data	Fresno Residential	14.9	4.94	63	0.95
Cool	Fresno Residential	30.7	4.78	36	0.94
Warm	Fresno Residential	-8.1	6.64	27	0.56
Cool	Helm	54.7	4.66	24	0.78
Cool	Kettleman City	35.7	4.60	23	0.94
Cool	Livermore	17.7	4.48	26	0.90
Cool	Merced	78.5	5.39	24	0.77
Cool	Modesto	13.6	4.95	22	0.98
Cool	Oildale	18.1	4.49	11	0.87
All Data	Olancha	1.4	3.08	52	0.64
Warm	Olancha	0.9	4.47	23	0.97
All Data	Pacheco	16.7	5.24	55	0.83
Cool	Pacheco	18.6	5.26	27	0.85
Warm	Pacheco	31.9	-0.42	28	
All Data	Pixley Wildlife	31.7	4.36	63	0.84
Cool	Pixley Wildlife	66.2	4.02	39	0.85
Warm	Pixley Wildlife	15.2	2.97	24	0.24
Cool	Pleasant	17.3	6.31	11	0.84
Cool	S.F.	-2.7	5.47	8	0.84
All Data	Sierra Nevada Foothills	-8.0	6.81	56	0.79
Cool	Sierra Nevada Foothills	1.1	6.73	28	0.82
Warm	Sierra Nevada Foothills	5.9	3.40	28	0.28
All Data	Selma Airport	18.1	5.50	64	0.88
Cool	Selma Airport	51.2	5.01	36	0.84
Warm	Selma Airport	-16.5	7.20	28	0.86
Cool	Stockton	19.2	4.70	24	0.81
Cool	Southwest Chowchilla	39.8	5.16	23	0.94
All Data	Tehachapi Pass	10.5	5.04	52	0.48
Cool	Tehachapi Pass	9.6	5.02	27	0.64
Warm	Tehachapi Pass	10.5	5.21	25	0.18
Cool	Visalia	81.7	4.16	24	0.80

This page is intentionally blank.